

Final Technical Report

ACTIVE DEFORMATION AND EARTHQUAKE POTENTIAL OF THE SOUTHERN LOS ANGELES BASIN, ORANGE COUNTY, CALIFORNIA

Award Number: 04HQGR0078

Recipient's name: Regents of the University of California - Irvine
Office of Research Administration
4199 Campus Drive, Suite 300
Irvine, CA 92612

Principal investigator: Lisa Grant, Ph.D.
Program in Public Health
101 Theory, Suite 250
University of California
Irvine, CA 92697-3957
lgrant@uci.edu

Program element: Research on earthquake occurrence and effects

Research supported by the U.S. Geological Survey (USGS), Department of the Interior, under USGS award number 04HQGR0078. The views and conclusions contained in this document are those of the authors and should not be interpreted as necessarily representing the official policies, either expressed or implied, of the U.S. Government.

TABLE OF CONTENTS

Cover Page

Table of Contents

Technical Abstract

Non-Technical Abstract

1. INTRODUCTION

- 1.1 Purpose, scope and publications**
 - 1.1.1 BIBLIOGRAPHY OF PUBLICATIONS RESULTING FROM WORK PERFORMED**
- 1.2 Research questions and tasks**
- 1.3 Orange County and the Southern Los Angeles Basin**
- 1.4 The Santa Ana Mountains and Puente Hills**

2. METHODS

- 2.1 Fluvial network analysis and age control**
- 2.2 Optically Stimulated Luminescence (OSL) Dating**
 - 2.2.1 OSL Sampling and Technical Details**

3. RESULTS

- 3.1 Results of OSL dating and stream terrace mapping**
- 3.2 Santa Ana River terraces at Burrell Ridge, Orange-Olive**
- 3.3 Santa Ana River and Santiago Creek sediments in the city of Orange**
- 3.4 Stream terraces in the Santa Ana River canyon**
 - 3.4.1 Age of Santa Ana River Terraces
- 3.5 Stream terraces along Santiago Creek in Santa Ana Mountains**
 - 3.5.1 Age of Santiago Creek Terraces
- 3.6 Uplift rates**

4 DISCUSSION

- 4.1 Uncertainty in ages and resulting uplift rates**
- 4.2 Basin Analysis**
 - 4.2.1 Puente Hills Basin Analysis**
 - 4.2.2 Santa Ana Mountains Basin Analysis**
- 4.3 Summary and Neotectonic model**

REFERENCES

Award number: 04HQGR0078

ACTIVE DEFORMATION AND EARTHQUAKE POTENTIAL OF THE SOUTHERN LOS ANGELES BASIN, ORANGE COUNTY, CALIFORNIA

Lisa B. Grant (P.I.), Program in Public Health, 101 Theory, Suite 250, University of California, Irvine, CA, 92697-3957; tel: 949-824-2889, fax: 949-824-0529, lgrant@uci.edu
Eldon M. Gath, Dept. of Environmental Health, Science and Policy, University of California, Irvine, CA, 92697-7070; gath@earthconsultants.com

TECHNICAL ABSTRACT

The main objective of this research is to investigate the rate and style of tectonic activity in the southern and eastern Los Angeles structural basin that is a source of poorly constrained seismic hazard for Orange County, California. This report is an expanded and updated version of prior Technical Reports (01HQGR0117 and 03HQGR0062 submitted by Grant) and unpublished dissertation research by Gath. Gath's dissertation presents a neotectonic model for the geomorphic development of Orange County, including the San Joaquin Hills (SJH), Santa Ana Mountains (SAM), Loma Ridge (LM), and Puente Hills (PH). In this model, the SAM became emergent approximately 3-4 Ma at a rate of 0.2-0.7 mm/yr. LR formed 2.5 Ma and blocked northern SAM drainages from flowing directly to the ocean. LR is interpreted as a southwest-vergent structure, obliquely accommodating north-south crustal shortening, initiating when the southern Newport-Inglewood fault (NIF) terminated into a right-stepping horsetail splay (consisting of the Cristianitos, Mission Viejo and Dana Cove faults). In the mid-Quaternary, the NIF stepped westward onto the Northern NIF branch, resulting in the compressional step that formed the SJH, a north-vergent, anticlinally deformed structure, bounded on the east by the Dana Cove fault, driven by strain partitioning off of the NIF, emergent less than 1 Ma, and uplifting at 0.25 mm/yr since 122 ka. At 200-300 ka, the NIF straightened into the LA Basin along the Southern NIF branch, producing uplift of Signal Hill, eliminating the source of compressive strain for the LR anticline. The PH became emergent 500-700 ka at 0.8 mm/yr, by uplift along the PH blind thrust fault (PHBTF). The PHBTF is accommodating N-S compressional strain, while the right-lateral Whittier fault is accommodating 2-3 mm/yr of NW vergent lateral strain of the Elsinore fault's (EF) 5-6 mm/yr slip. The Coyote Hills are an en-echelon series of hanging wall folds similar to LR, caused by thrusting the SAM block into Santa Ana River (SAR) sediments, using the PHBTF as a decollement. The Chino fault, a right-lateral extension of the EF, accommodates 1-2 mm/yr motion, which results in an EF strain surplus of 1-3 mm/yr for uplift of the SAM. The Peralta Hills fault, an EF backthrust, deflects the SAR 3 km westward by uplift of LR. The regional deformation is driven by the SAM moving northwest as an "indenter" and compressing the soft sedimentary fill in the eastern Los Angeles basin. The indenter is being driven northwestward at a rate of approximately 6 mm/yr along the EF. Due to inertia and pinning by the NIF and SJH thrust, the onlapping sedimentary deposits on the southwestern side of the SAM are being underthrust and deformed by movement of the SAM batholith. Deformation is accommodated by compressional folding of LR, and a left-lateral shear zone along Santiago Creek and the SAM foothills. Shearing has caused 3 km deflections of Santiago Creek due to drag and block rotation. Approximately 12-15 km total displacement along the zone is estimated from apparent offset of the Holz Shale. According to this model, dextral strain at a rate of 6 mm/yr along the EF should be balanced by sinistral shearing (along

the 4-S Ranch and other faults) and by block rotations along the southwestern side of the SAM indentor. Block rotations are likely accommodated through reactivation of Miocene normal faults (Mission Viejo, Cristianitos, Dana Point, Bee Canyon, El Modena, and unnamed N-S trending faults) that formed during Borderlands extension. This neotectonic model implies that seismic hazard in Orange County is higher than previously estimated because there is a previously unrecognized zone of distributed deformation in southeastern Orange County.

NON-TECHNICAL ABSTRACT

The main objective of this research is to better understand seismic hazard in Orange County, California, an area of nearly 3 million people. This project investigates possible tectonic uplift and earthquake potential associated with tectonic processes and undiscovered faults in or near the Santa Ana Mountains and Puente Hills by examining the age and elevation of stream deposits. The Santa Ana Mountains are prominent features in the landscape of the metropolitan Los Angeles basin. Comparable sized mountains and foothills in surrounding areas are known to be associated with active faults. Results indicate that the Santa Ana Mountains are rising, most likely in association with movement of active faults.

1. INTRODUCTION

1.1 Purpose, scope and publications

This report is an expanded and updated version of prior Technical Reports (01HQGR0117 and 03HQGR0062 submitted by Grant) and unpublished dissertation research by Gath. FTR 03HQGR0062 (Grant et al., 2006) summarized preliminary results of studies of the distribution, age and neotectonic significance of fluvial terraces along the Santa Ana River and Santiago Creek in the eastern Puente Hills (PH) and northern Santa Ana Mountains (SAM). The terrace data and portions of the analysis sections are reprinted in this report for completeness. A preliminary neotectonic model for the eastern PH and SAM presented in the previous report has been significantly revised for this report. This report also contains revised basin analysis data from Final Technical Report 01HQGR0117 (L. Grant, PI) referenced herein as Gath et al. (2002).

The principle objective of this long-term research is to better understand the neotectonics and seismic hazard in Orange County, southern California, to promote seismic hazard mitigation and planning. The research builds on related work funded by USGS to study the Whittier fault in the Puente Hills (Gath, 1997), and more recent tectonic geomorphology study of the southern Los Angeles basin (Gath et al., 2002; Grant et al., 2006). Comprehensive results will be published in a doctoral dissertation by Eldon Gath at UC Irvine. Related research on the San Joaquin Hills and southern Newport-Inglewood fault zone has been published in journal articles (Grant et al., 1997, 1999, 2000, 2002; Grant and Rockwell, 2002). Preliminary results have been presented in abstracts and a field trip guidebook listed below

1.1.1 BIBLIOGRAPHY OF PUBLICATIONS RESULTING FROM WORK PERFORMED

- Gath, E. M and Grant, L. Quaternary geomorphic development and seismic hazards of Orange County, southern Los Angeles basin, California (2007). AAPG 2007 Annual Meeting, April 1-4, Long Beach, CA.
- Gath, E. M., Grant, L. B. and Gath and Owen, L. A. (2006). Temporal Controls on Uplift and Slip Rates for the Puente Hill and San Ana Mountains, Southern Los Angeles Basin, Orange County, California. 2006 AGU 2006 Fall meeting, December 11—15, San Francisco, CA. Abstract T13B-0514
- Gath, E. M. and L. B. Grant (2004). Learning from Northridge: A progress report on the active faults of Orange County, *Seism. Res. Ltrrs.*, 75 (2), March/April, p. 260.
- Gath, E. M. and Grant, L. B. (2002). Is the Elsinore fault responsible for the uplift of the Santa Ana Mountains, Orange County, California? GSA Abstracts with Programs, v. 34, no. 5, April, p. A-87, 2002.
- Gath, E. M., Runnerstrom, E. E. and L. B. Grant (PI) (2002). Active deformation and earthquake potential of the southern Los Angeles basin, Orange County, California. U.S. Geological Survey National Earthquake Hazard Reduction Program, Final Technical Report, Award Number 01HQGR0117.
- Gath, E., L. Grant and E. Runnerstrom (2003a). Using strike-slip offsets for temporal control of the development of a Quaternary drainage network in southern California, (abs) Program with Abstracts, Association of Engineering Geologists, 2003 Annual Meeting, AEG NEWS, v. 46, p. 56.
- Gath, E., L. Grant, and L. Owen (2003b). Temporal controls on vertical motion rates for the Santa Ana Mountains and Puente Hills, Orange County, California, Proceedings and Abstracts, v. XIII, SCEC Annual Meeting, p.88.
- Grant, L. B., Gath, E. M., Owen, L. A. and E. E. Runnerstrom (2006). Active deformation and earthquake potential of the southern Los Angeles basin, Orange County, California, in "Geology of the Orange County Region, Southern California, Field Trip Guidebook No. 33, J. Bonsangue and R. Lemmer, (Eds)., South coast Geological Society, P. O. box 10244, Santa Ana, CA 92711-0244, p. 101-134.
- Grant, L. B., Gath, E. M., Owen, L. A. and E. E. Runnerstrom (2006). Active deformation and earthquake potential of the southern Los Angeles basin, Orange County, California, Final Technical Report, U. S. Geological Survey, Department of the Interior Award Number 03HQGR0062.

Grant, L. B., and Rockwell, T. K. (2002). A Northward propagating earthquake sequence in coastal southern California? *Seismological Research Letters*, v. 73, no. 4, p.461-469, 2002.

1.2 Research questions and tasks

The major questions addressed by our long-term research are:

- What are the significant sources of seismic hazard in the southern Los Angeles basin (Orange County, California)?
- What are the rates and styles of active deformation?
- What does deformation in the southern LA basin reveal about regional neotectonics and seismic hazard?

The specific tasks required to address these questions are: 1) map the location and spatial pattern of geomorphic features that are indicative of active faulting; 2) obtain ages of key sediments and geomorphic surfaces; 3) analyze the temporal and kinematic relationships of those features; 4) develop a tectonic model to explain the observed deformation; and 5) communicate these results to achieve improved loss reduction practices in industry, local government, and the citizens of Orange County. The first four tasks are accomplished by integrating Quaternary geology with geomorphic mapping to identify active tectonic structures by their effect on the evolution of the landscape, especially as reflected in the development patterns of the stream systems. The fifth task is a much longer-term goal.

Recent research focused on tasks 3 and 4. For completeness, this report describes results of tasks 2, 3 and 4.

1.3 Orange County and the Southern Los Angeles Basin

Orange County is coincident with the southern Los Angeles basin. It is developing rapidly and becoming a high technology center of national significance. Three million people live and work in the area shown on Figure 1; at least double that many would be impacted by earthquakes with an epicenter in the southern Los Angeles Basin. Orange County is especially vulnerable to earthquake damage because the hazard is perceived to be relatively low (Figure 2) and seismic hazard mitigation measures have been less stringent than in some other areas of the Los Angeles basin and surrounding region. Of concern is the possibility that the Orange County hazard is the same as farther north in Los Angeles, only not recognized as such.

The southern Los Angeles basin study area is bounded on the north by the eastern Puente Hills, on the east by the northern Santa Ana Mountains, on the south by the San Joaquin Hills and San Juan Creek, and on the west by the Pacific Ocean (Figure 1). The Los Angeles basin initially formed as a result of late Miocene extension along low angle detachment faults (Crouch and Suppe, 1993). Approximately 2-3 Ma, the basin began to close in response to the development of the San Andreas fault. The Los Angeles basin now occupies the transition from strike-slip dominated tectonics to the south, to Transverse Ranges thrust tectonics to the north. South of the Transverse Ranges, structural modeling suggests that the Los Angeles basin is underlain by a complex network of blind thrust faults (Davis et al., 1989; Hauksson and Jones, 1989; Hauksson, 1990; Shaw, 1993, Shaw and Shearer, 1999) that may be a reactivation of the Miocene

detachment faults. These thrust faults have generated much of the recent seismic activity in the basin (Whittier Narrows M5.9 in 1987 and Northridge M6.7 in 1994).

Seismic hazard in the Orange County area has long been assumed to be low (Petersen and Wesnousky, 1994; WGCEP, 1995, Petersen et al., 1996). With the exception of the 1933 Newport-Inglewood fault's, M6.3 "*Long Beach*" earthquake, which actually occurred in the northern Newport Beach area at the southwest margin of the LA Basin (Hauksson and Gross, 1991), no significant historical seismicity has occurred in this region. The San Joaquin Hills, eastern Puente Hills, Santa Ana Mountains, and surrounding regions have been essentially devoid of significant (>M5) earthquakes during the historic period. In contrast, damaging earthquakes have occurred farther north in the Los Angeles region and in the Transverse Ranges, generating intense scientific interest and research in these tectonically active areas. However, recent research shows that several unrecognized (Gath et al., 2002) or recently recognized (Grant et al., 1999, 2002; Dolan et al., 2003; Shaw and Shearer, 1999; Shaw et al., 2002) tectonically active and potentially seismogenic faults exist in the southern Los Angeles basin. The general lack of seismicity in this region may be the result of these faults being locked and only releasing strain in large earthquakes, rather than to the absence of seismogenic sources.

1.4 The Santa Ana Mountains and Puente Hills

Rising to a height of over 1,700 meters above sea-level, the Santa Ana Mountains (SAM) are the northernmost extent of the California Peninsular Ranges (Figure 3) at the southeast margin of the Los Angeles basin. They rise nearly 900 meters above the heavily populated urban centers in Orange and Riverside Counties, but neither their uplift rate nor uplift mechanism has been determined. The SAM are the dominant landform in southern Orange and western Riverside County, yet they have not been included in seismic hazard models. This research presents an initial analysis of late Quaternary tectonic uplift of the Santa Ana Mountains as a first step towards quantifying the seismic hazard.

The Puente Hills are an uplifting range of hills (Figures 1, 3 and 4) composed almost exclusively of the Puente Formation, a Miocene-age marine sequence of deepwater sandstone and shale (Durham and Yerkes, 1964; Yerkes, 1972). The Puente Hills (Figure 4) are the surface expression of the south vergent, Puente Hills thrust (Shaw and Shearer, 1999; Shaw et al., 2002). Paleoseismic investigations of this blind structure present evidence for 1-2 meters of uplift approximately every 1500-2500 years since the early Holocene (Dolan et al., 2003.). Cutting through the foothills of the Puente Hills is the Whittier fault, a right-lateral, strike-slip fault, that is transferring the Elsinore fault's 5 ± 1 mm/yr strain directly into the Los Angeles basin (WGCEP, 1995). The southern flank of the Puente Hills has a well-ordered fluvial drainage network consisting of primary trunk streams and hundreds of tributary streams. In the western half of the Puente Hills, periodic stream capture has complicated the drainage history, but in the eastern half the drainage basins are all distinct and separable. This research focuses on the eastern half of the Puente Hills.

All streams crossing the Whittier fault are right-laterally deflected at a rate of 2-3 mm/yr, as measured by 3-D paleoseismic trenching (Gath et al., 1992; SCEC, 1995; Gath and Rockwell, in prep.). Gath (1997) observed that the larger streams were displaced greater amounts than the smaller streams, indicating a temporal relationship of progressive growth faulting. The distance

that a stream has been offset can be used as a proxy for the age of the stream by dividing the offset by the rate of slip on the fault. Late Quaternary ages of offset streams were derived from the Holocene slip rate of 2-3 mm/yr (WGCEP, 1995) and presented by Gath (1997) and Gath et al. (2002).

Gath (1997) proposed that the Puente Hills were being uplifted by a blind Elysian Park thrust, while the Coyote Hills series of anticlinal folds were the result of compressive strain partitioned off of the Whittier fault, similar to the Bullard and Lettis (1993) model for the Montebello Hills. Preliminary research by Gath (1997) suggested that the Puente Hills have been rising tectonically at a rate of 0.5-0.6 m/ka since ~ 1 Ma. Shaw and Shearer (1999) modeled this uplift as a new blind thrust fault (the Puente Hills fault). The late Quaternary uplift rate of the eastern Puente Hills is addressed in this report. The uplift rate is derived from ages and elevations of fluvial terraces in the Santa Ana River canyon along the southeastern margin of the Puente Hills.

Youthful topography and preliminary analysis of its fluvial systems indicate that the Santa Ana Mountains are also tectonically uplifting at a relatively rapid rate (Gath et al., 2002, 2003a,b; Gath and Grant 2004). This uplift is hypothesized to be in response to termination of the Elsinore fault and consumption of some of its strain into uplift (Gath and Grant, 2002). The Elsinore fault's 5-6 m/ky strain (WGCEP, 1995; Lamar and Rockwell, 1986; Hull and Nicholson, 1992) is partially transferred to the Whittier fault (2-3 mm/yr; Gath et al., 1992), and the Chino fault (~1-2 mm/yr; Walls and Gath, 2001). The remaining strain, or "slip deficit" is most likely responsible for uplift of the Santa Ana Mountains and Loma Ridge in the foothills of the Santa Ana Mountains.

Loma Ridge is a northwesterly trending structure, parallel to the Santa Ana Mountains (SAM). It forms the foothills of the SAM south of Santiago Creek, and is cross-cut by several N-S trending strike-slip faults (Morton and Miller, 1981) that consistently deflect Santiago Creek 2000 m northerly (in an upstream direction), but do not appear to affect the dissected range front in the Irvine foothills (Gath et al., 2003). The activity of the N-S faults is uncertain, but they appear to be (or have been) accommodating lateral strain on the hanging wall of an oblique, blind thrust under Loma Ridge (and the northern Santa Ana Mountains).

A series of elevated fluvial terraces along Santiago Creek suggest late Quaternary uplift of the SAM and provide the opportunity to measure tectonic uplift of the Santa Ana Mountains and Loma Ridge.

2. METHODS

2.1 Fluvial network analysis and age control

Many studies have demonstrated that examination and analysis of fluvial system development patterns can be applied to quantify neotectonic deformation (e.g., Ohmori, 1993; Montgomery, 1994; Nicol et al., 1994; Pazzaglia et al., 1998; Kirby and Whipple, 2001). Profiles of channels and elevated terraces contain information about deformation rates and patterns. In a study to determine the rate of regional uplift, Merritts et al. (1994) mapped the long channel profiles of elevated fluvial terraces to determine the evolution of the channel profile, also referred to as "grade," through time. Cox (1994) used an asymmetric pattern of drainage system evolution as a

proxy to indicate the regional tilting and tectonic deformation. Bullard and Lettis (1993) mapped elevated geomorphic surfaces and a pattern of channel abandonment to reveal subsequent deformation and model the pattern of uplift by a localized blind thrust fault. Rosenbloom and Anderson (1994) measured longitudinal channel profiles of rivers cut through elevated marine terraces on a progressively uplifting mountain range to correlate residual river knickpoints with marine terrace elevations. This indicated that bedrock channels fail to fully regrade after pronounced base level lowering, and thus preserve a record in their longitudinal profile of the eustatic cycles to which they have been subjected. In the southern Los Angeles basin marine terraces and stream terraces can be correlated with eustatic sea level cycles to constrain tectonic uplift rates (Grant et al., 1999; Gath et al., 2002).

The magnitude of the interglacial-glacial base level changes in a near-coastal fluvial system overwhelms typical tectonic processes, and such base level change is the likely origin of major synchronous terrace surfaces (Personius, 1993). In the absence of other supporting age control, such a conclusion is speculative. However, in the Los Angeles basin there are sufficient data to show that eustatic fluctuations are the dominant terrace-forming events because of their close association to the marine terraces in the uplifted areas (Grant et al., 1999) and to stratigraphic unconformities in the basin areas (Ponti et al., 1986 & 1991). Correlation of terraces with global eustatic sea level changes provides constraints on the age of terrace surfaces. There is a suite of elevated Santa Ana River terrace deposits within the eastern Puente Hills. These terraces have been incised by the southerly draining streams, but the terraces were the local base level at the time the streams were first formed because they were all tributary to the Santa Ana River drainage. Therefore, the approximate age of the terraces can be inferred from correlation with eustatic sea level changes.

In tectonically active areas, stream terrace formation and abandonment is also affected by tectonic deformation. The Whittier fault trends N65°W across the lower foothills of the Puente Hills (Figure 4), and has right-laterally offset streams crossing the fault (Gath, 1997). Streams lengthen with time, and in the Puente Hills, these streams are increasingly offset by the Whittier fault. Therefore, these offsets can be used to provide temporal control on the rate of other geomorphic processes occurring within the Puente Hills. By retrodeforming the offset streams at the 2-3mm/yr rate of slip on the fault [dividing the total stream offset by the fault slip rate] we can calculate the age of the stream before it was initially offset by the fault (Gath et al., 2002, 2003a). Offsets range from 4 m to 3000 m (Gath, 1997). Major drainages in the eastern Puente Hills are offset 248 - 1676 m and range in age from 99 ka to 670 ka, assuming a constant slip rate of 2.5 m/ka (Gath et al., 2002).

The ages derived from tectonic offset, correlation with sea level and climatic change can be compared with estimates of age of soils developed on the terrace surfaces. A fourth independent method is Optically Stimulated Luminescence (OSL) dating. OSL dating works by dating the time of burial of sandy (quartz-rich) sediments. We sampled terraces in the Santa Ana River and Santiago Creek for OSL dating.

2.2 Optically Stimulated Luminescence (OSL) Dating

Optically stimulated luminescence (OSL) dating is used to determine the time elapsed since a sediment sample was exposed to daylight. This technique has been successfully applied to dating deformed sediments for paleoseismic studies in the western USA (e.g. Machette *et al.*, 1992; Crone *et al.*, 1997; Rockwell *et al.*, 2000; Lee *et al.*, 2001; Kent *et al.*, 2005; Wesnousky *et al.*, 2005) and elsewhere in the world (e.g. Owen *et al.*, 1999; Washburn *et al.*, 2001). The technique relies on the interaction of ionizing radiation with electrons within semi-conducting minerals resulting in the accumulation of charge in metastable location within minerals. Illuminating the minerals and detrapping the charge that combines at luminescence centers can determine the population of this charge. This results in the emission of photons (luminescence). Artificially dosing sub-samples and comparing the luminescence emitted with the natural luminescence can determine the relationship between radiation flux and luminescence. The equivalent dose (D_E) experienced by the grains during burial therefore can be determined. The other quantity needed to calculate the age is the ionizing radiation dose rate, which can be derived from direct measurements on measured concentrations of radioisotopes. The age is then derived using the equation:

$$\text{Age} = D_E / \text{dose rate}$$

Uncertainty in the age is influenced by the systematic and random errors in the D_E values and the possible temporal changes in the radiation flux rate. The quoted error is the deviation of the D_E values on multiple sub-samples and the error in measured ionizing radiation dose rate or the concentration of radioisotopes.

It is not possible to determine temporal changes in the dose rate that is a consequence of changes in water content and the growth and/or translocation of minerals within the sediment. *The dose rate is therefore generally assumed to have remained constant over time and results presented in this report are derived assuming a constant dose rate.* The environment of deposition and its possible effect on dose rate of the samples may be considered in interpreting results, especially if it appears that conditions might have changed significantly due to changes in climate or geologic processes. To account for possible changes in moisture conditions, two ages were calculated for each sample based on assumed water content of $10 \pm 5\%$ and $15 \pm 5\%$.

2.2.1 OSL Sampling and Technical Details

In 2003 and 2004 we collected 16 samples from Santa Ana River stream terraces in the Puente Hills and Peralta Hills, from Santiago Creek terraces in the Santa Ana Mountains, and from the confluence of the Santiago Creek and Santa Ana River floodplains in the city of Orange. Samples were processed by Professor Lewis Owen at University of Cincinnati. Locations of samples and descriptions of terraces are in following sections. Three samples were destroyed in laboratory mishaps.

Sediment samples for OSL dating were collected by hammering light-tight tubes into freshly exposed sediments. The tubes remained sealed until processed in the safe light conditions in the laboratory. The *in situ* water content (mass of moisture/dry mass; Aitken, 1998) was determined using sub-samples and drying them in an oven at 50°C. The sample for dating was dry sieved to obtain a 90-125 μm particle size fraction. The carbonates and organic matter were removed from the 90-125 μm fraction using 10% HCl and 30% H_2O_2 , respectively. Sodium polytungstate

solutions of different densities and a centrifuge were used to separate the quartz and feldspar-rich fractions from the heavy minerals. The separated quartz-rich fraction was treated with 49% HF for 80 minutes to dissolve any plagioclase feldspars and remove the alpha-irradiated surface of the quartz grains. Dried quartz grains were mounted on stainless steel discs with silicon spray. All the preparation techniques were carried out under laboratory safelights to avoid sample bleaching.

Approximately 20 g of the dried sub-sample from the sediment sample was ground to a fine powder and sent to the Becquerel Laboratories at Lucas Heights in Australia for neutron activation analysis (INAA). Using dose-rate conversion factors of Adamiec and Aitken (1998) and beta attenuation factors of Mejdahl (1979) and Adamiec and Aitken (1998), the elemental concentrations were converted into external beta and gamma components, which were in turn attenuated for moisture content. These were summed together with a cosmic ray component using the methods of Prescott and Hutton (1994) to give estimates of the total dose-rate for each sample.

Variable water content throughout the section may have occurred throughout the history of the section. However, it is not possible to determine the degree of such changes and we have assumed that the dose rate has remained constant, but have used $10 \pm 5\%$ and $15 \pm 5\%$ water content to help account for possible changes in water content. The INAA, cosmic dose rates, total doses, are shown in Table 1. The dose rates are well within the normal range for natural dose rate.

Luminescence measurements were undertaken using a Daybreak 1100 automated system with an 1100FO/L combined fiber-optic/IRLED illuminator for optical stimulation (Bortolot, 1997). Luminescence from the quartz grains was stimulated using a 150 W halogen lamp producing green light ($514\Delta 34$ nm; ~ 20 mWcm⁻²) defined by an additional narrow band interference filter. All quartz samples were screened for feldspar contamination using infrared stimulation from T-1 GaAlAs diodes ($880\Delta 80$ nm; diode current 20 mA). All OSL signals were detected with a photomultiplier tube characterized by 9 mm Schott UG11 ultraviolet detection filters. Daybreak TLApplic 4.30 software was used for hardware control and D_E analysis.

D_E measurements were determined on multiple aliquots for each sample using the SAR protocol developed by Murray and Wintle (2000). In the SAR method, each natural or regenerated OSL signal is corrected for changes in sensitivity using the OSL response to a subsequent test dose. The natural dose (N) was measured in the first cycle, and thereafter five regeneration doses (R₁ to R₅) were administered. The first three were used to bracket the natural luminescence level (R₁ < N ~ R₂ < R₃), the fourth (R₄) was set at zero to monitor recuperation (i.e. R₄/N) and to monitor the reproducibility of sensitivity corrections the fifth dose was made that had an equal to the first dose (i.e. R₅/R₁). Each measurement cycle comprised a regeneration dose (zero for natural), preheating of 220°C for 10 s, optical stimulation for 100 s (sample temperature of 125°C), a constant test-dose, a test-preheat of 160°C for 0 s and a final optical stimulation for 100 s (at 125°C). The net-natural and net-regenerated OSL were derived by taking the initial OSL signal (0-1 s) and subtracting a background from the last part of the stimulation curve (90-100 s); subtracting the background from the preceding natural and regenerative OSL signals

derived the net test-dose response. Growth curves were plotted using the net natural and regenerated data divided by the subsequent response to the net-test dose. The growth curve data was fitted with a single saturating exponential.

3. RESULTS

3.1 Results of OSL dating and stream terrace mapping

Results of OSL dating are displayed in Table 1. Elevations shown in Table 1 are sample elevations from a handheld GPS receiver. The GPS elevations of each sample were compared with topographic quadrangle maps (20 foot contour interval) in the field, and corrected if appropriate. Corrected sample elevations are displayed in Table 2. In most cases, the sample elevations differ from the elevations of the terrace surfaces because the samples were collected within the terrace fill below the terrace surface. Table 2 provides approximate elevations of terrace surface corresponding to each sample, and the estimated elevation of local base level.

The D_E for each sample was calculated using the mean values and standard error of all the aliquots for each sample (Table 1). A large spread of D_E values may reflect partial bleaching of sediment. This would result in an overestimate of the true age of the sediment. Therefore the ages presented in Table 1 could be maximum ages for the timing of sediment deposition, assuming that the water content and dose rate were constant. However, dose rates may have varied due to climate change and the resulting change in water and clay content of the terrace sediments. Ages were calculated for each sample based on assumed water content of $15 \pm 5\%$ for wetter glacial conditions, and $10 \pm 5\%$ for drier conditions and/or interglacial periods. Results of both calculations are displayed in Table 1.

In sample LG4, the D_E values exceeded 300 Gy for most aliquots. Since the regenerative growth curves became highly sub-linear after about 250 Gy for sample LG4, it was not possible to calculate precise D_E values for these aliquots. The minimum D_E values are used to calculate a minimum age of 75 ka, although the true age is likely to be significantly higher.

3.2 Santa Ana River terraces at Burrell Ridge, Orange-Olive

Samples LG4 and LG5 were collected from the first fluvial terrace at Olive on the flank of Burrell Ridge in the city of Orange. (See Figure 5 for map and Figure 6 for photo.) In this area, the Santa Ana River is deflected westerly by growth of the Olive anticline and Burrell Ridge in the Peralta Hills at the westernmost tip of Loma Ridge (Gath et al., 2002). This growth is accommodated by the Peralta Hills fault (Bryant and Fife, 1992; Whitney and Seymour, 1992; Schoellhamer et al., 1981), geomorphically expressed as a 3 meter fold or fault scarp in alluvium approximately 100 meters south of the sample location. The surface of the terrace at 116 m elevation is 55 meters above the local Santa Ana River base level. Below the elevated terrace is a large alluvial fan surface grading to the SAR. As the first emergent terrace above the Santa Ana River, we mapped this terrace as the lowest regional terrace, Qt1 prior to dating. However, it does not appear to be a regional terrace, but rather the westernmost extent of the Olive anticline above the SAR. The age of this terrace would be indicative of the uplift rate of the Olive anticline and the slip rate of the Peralta Hills fault, and it would not necessarily correlate other than

temporally, with the Puente Hills terraces farther east up Santa Ana Canyon. Two OSL samples were collected from sediments comprising the lowest terrace where the Olive Anticline terminates westerly at the modern river floodplain level. One sample (LG5) was compromised in a lab accident, and analysis of the second sample (LG4) indicates an age of at least 75 ka. The sample could be significantly older than 75 ka. Thus, this terrace is probably correlative with the marine oxygen isotope stage 5e terraces mapped regionally within the study area. The well developed soil upon the terrace further supports this interpretation.

3.3 Santa Ana River and Santiago Creek sediments in the city of Orange

Samples EG1 and EG2 were collected in a road cut along the 22 Freeway approx. 200 m west of the intersection with the 55 Freeway. Elevation of sample EG1 was approx. 1 m higher than sample EG2 and therefore EG1 was expected to be younger than EG2. The samples were collected from an alluvial fan of Santiago Creek which prograded onto the floodplain of the Santa Ana River. The age of the samples constrain the approximate time since the Santa Ana River captured Santiago Creek. The age of the samples suggests that stream capture occurred approximately 4-6 ka. The timing of stream capture is important for understanding the regional geomorphology and Holocene tectonic evolution of the Santa Ana Mountains, San Joaquin Hills, and Puente Hills. This will be explored in greater depth in forthcoming Final Technical Report for 04HQGR0078.

3.4 Stream terraces in the Santa Ana River canyon

Through the Santa Ana River canyon, the Puente Hills exhibit a suite of fill terraces and strath surfaces that have been preserved by uplift of the Puente Hills. A suite of at least four fill terraces created by the Santa Ana River are inset within Santa Ana Canyon (Gath, 1997). These terraces are dominated by deposits of coarse gravels and cobbles, with occasional lenses of sand. At higher elevations across the entire Puente Hills are at least three regionally-broad, erosional, strath surfaces (Gath et al., 2002) (Figure 7). Detailed mapping and correlation of strath surfaces and inset fill terraces provide a map of the pattern of uplift and deformation within and across the Puente Hills. Figure 8 shows these terraces within the Santa Ana Canyon area of the eastern Puente Hills. The isolated terraces are correlated into broad bands similar to the San Joaquin Hills terraces.

Fill Terrace 4, Qt4, at a height of 760-800 feet lies about 400 feet above the modern Santa Ana River. The terraces are expressed as small remnants of fluvial cobble and sand deposits on the noses of the interfluvial ridgelines. Terrace 4 has a terminal soil developed on the terrace surface, indicating an age of probably 200 ky or greater.

Fill terrace 3, Qt3, at a surface elevation of about 630-700 feet (Figure 9), is the principal elevated surface throughout the region, and is the terrace into which Box, Bee, and Yorba Canyons are incised. Terrace 3 is formed by approximately 30 meters of upwardly fining deposits; basal gravels and cobbles, clean sands, and silty overbank deposits comprise the fluvial package, that is then capped by locally-generated, crudely stratified, fan and mudflow deposits.

The intermediate terrace, Qt2, is geomorphically well expressed in the Santa Ana River canyon on both the Puente Hills and northern Santa Ana Mountains sides of the river. Samples LG7, LG10 and LG11 were collected from terrace Qt2, as shown on the map in Figure 8 and photos in Figures 10 and 11.

The lowest terrace, Qt1 (photos in Figures 12 and 13), is dominantly conglomeratic, and has a moderately well developed soil profile. Samples LG6, LG8 and LG9 were collected from Qt1 at sites shown on Figure 8. Terrace 1, Qt1, is inset into the toe of Terrace 2, Qt2.

The surface of terrace Qt1 is 14-46 m above equivalent modern base level of the Santa Ana River (Table 2, samples LG6, LG8, LG9), indicating that it, and other higher terraces, have been uplifted since deposition as part of the Puente Hills block. The surface of a second terrace, Qt2, is approx. 15 m above Qt1, and 33 - 38 m above baselevel, as defined by the Santa Ana River (Table 2, samples LG7, LG11).

3.4.1 Age of Santa Ana River Terraces

Stream terraces form over relatively long time periods in response to climate change and/or tectonic processes. In coastal areas, the preferred model is that fill terraces were deposited during eustatic sea level high stands, incised by river response to low stands, and preserved by uplift in the intervening low-stands. Thus the terrace surfaces can be approximately dated by correlating with the age of the transition from a eustatic highstand to a lowstand. This close to the ocean, the time required for knickpoint (incision) migration would be minimal, compared to the age of the terrace, in a river as large as the Santa Ana.

Soil ages provide constraints on the length of time the terrace surface was exposed and stable. Climate change and local environment may affect soil age estimations. Based upon the Soil Profile Development Index of Harden (1982), Rockwell (Rockwell and others, 1988; 1992) determined an average age of 140 ± 70 ka for the Qt3 terrace surface in the Puente Hills, and a probable age of 200-240 ka for the basal terrace gravels. By extrapolation, Qt2 was estimated to be approximately 80 ka, and Qt 1 was estimated to be around 40 ka.

OSL dates for all samples are shown in Table 1. OSL dating provides age since deposition of sediment, with unknown adjustment required for change in dose rate due to change in environment, if any. OSL dates yielded consistent results between samples from the same terraces, but ages are younger than those derived by other methods. Possible explanations are discussed in section 4. We propose to consider OSL ages as minimum ages for terraces in Santa Ana River canyon.

Ages of the Puente Hills terraces can be estimated by applying 3 methods: correlating with eustatic sea level cycles, soil ages, and results of OSL dating. A fourth method is based on estimate of incision date, and amount of offset by the Whittier fault (Gath et al. 2002; Gath 1997). The largest drainage basins (Carbon, Tonner, and La Mirada) in the Puente Hills are all offset about 1,700 m (Gath, 1997). Using the Gath et al. (1992) slip rate of 2.5 mm/yr, these drainages incised ~ 700 ka, which is consistent with the age of the second geomorphic surface estimated by correlating with sea-level highstands (Gath et al., 2002). Gath (1997) also

interpreted 2,700 m of deflection on the Santa Ana River and ~3,000 m of deflection on the San Gabriel River. Based on the 2.5 mm/yr slip rate, the age for the entrainment of these two trunk streams within the emerging Puente Hills is ~1,100-1,200 ka, which is consistent with the age extrapolated from the sea level correlation chart for the oldest erosional surface on the Puente Hills (Figure 7, Gath et al., 2002). Additionally, using the pedogenically-derived 120-140 ka age for the Qt3 surface, and the average 400 m offset of the streams incised into those surfaces (Box, Blue Mud, Lost Trough, Lomas de Yorba) by the Whittier fault, yields a similar magnitude (2.8-3.3 mm/yr) slip rate for the Whittier fault, lending support to the pedogenic ages for the terraces.

Results of multiple dating methods are presented in Table 3. Preferred ages of terraces in Santa Ana Canyon are shown on Figure 14 and in Table 3. Preferred ages are in good agreement with ages of Santiago Creek terraces in the Santa Ana Mountains, as described in section 3.5.

3.5 Stream terraces along Santiago Creek in Santa Ana Mountains

Eight discrete geomorphic surfaces were identified on Loma Ridge and the Santa Ana Mountains (Gath et al., 2002). These are interpreted to be erosional and depositional surfaces created during past eustatic high stands, similar to those in the San Joaquin and Puente Hills. There are four fluvial fill terraces inset within Santiago Creek in the northern Santa Ana Mountains and the margins of Loma Ridge (Figure 15). At least three fill terraces are present on the flank of the Santa Ana Mountains along the north side of Santiago Creek (Figures 15 and 16).

Geomorphic analysis (Gath et al., 2002 and in prep.) shows that Santiago Creek is trapped between the uplifting Santa Ana Mountains and Loma Ridge. Although Santiago Creek would certainly have a response to the eustatic sea level fluctuations, it is likely that tectonic factors are at least partially responsible for terrace generation and preservation of elevated terraces along Santiago Canyon. As described in section 3.2, Santiago Creek was captured by the Santa Ana River during the mid-Holocene. Prior to that time, it might have flowed through Newport Bay. Its course may have been altered by uplift of the San Joaquin Hills or Loma Ridge, or both.

3.5.1 Age of Santiago Creek Terraces

The terraces are dated by OSL dating and correlation with sea level highstands. Preliminary terrace ages are shown in Table 4. Soil ages are not available for Santiago Creek terraces, although relative soil development was used to correlate terraces.

Age correlation of fill terraces is based in part on correlation of the strath surface at 70 m elevation with marine oxygen isotope stage 7 or 9 sea level highstand. This would be approximately equivalent to the lowest shoreline or erosional surface identified at the toe of Loma Ridge (Gath et al., 2002), consistent with the inferred closing of the embayment from previous studies of the San Joaquin Hills (e.g., Grant et al., 1999).

OSL dating yielded consistent results, with similar sediment ages of 64.3 ± 6.4 ka and 62.1 ± 7.1 ka for two sample locations [LG-1 and LG-2] taken only one meter apart near the base of the first emergent terrace (assumed to be Qt2) at Irvine Lake. OSL dating of the sediments near the top of a correlative terrace on the opposite side of Irvine Lake yielded an age of

53.7±4.9 ka. A similar age of 58.6 ± 5.5 ka was returned from a sample of the lowest emergent terrace Qt1(?) further downstream along Santiago Creek.

As shown in Table 4, the OSL ages are slightly younger than ages based on correlation with sea level highstands. Preferred ages of the terraces, shown in Table 4, are based on correlation with sea level highstands.

3.6 Uplift rates

For each sample, uplift rates can be calculated from OSL dates (minimum ages) and preferred terrace ages. Results are displayed in Table 5, with values for the Santa Ana Mountains and foothills in italics. The elevations of individual samples, and stream terraces are displayed in Tables 1 and 2. For calculating uplift rates, the relevant elevation is the difference between the height of a terrace surface, and local base level, as shown in column 4 of Table 5.

Uplift rates of the Santa Ana Mountains and foothills derived from Santiago Creek terraces range from 0.2 – 0.7 m/ka. These results are consistent with preliminary geomorphic analysis (Gath et al., 2002) showing that the Santa Ana Mountains are tectonically active.

Uplift rates of the Puente Hills range from 0.6 – 1.4 m/ka based on OSL dates, and 0.2 – 0.8 m/ka based on other methods. The rates overlap in the range 0.6-0.8 m/ka, and we propose that this is the most reliable estimate of uplift rate because it is based on several methods. An uplift rate of 0.6-0.8 m/ka for the Puente Hills is also consistent with preliminary results of geomorphic analysis (Gath et al., 2002).

4 DISCUSSION

4.1 Uncertainty in ages and resulting uplift rates

For the Puente Hills, the difference in ages between OSL dates and soil ages or sea level correlations is greater than expected. The most likely explanation is that dose rate has changed, and therefore OSL provides minimum ages. For the Puente Hills, OSL ages result in a doubling of the uplift rate over the pedogenic rate to 1.6 mm/yr, comparable to the Teton Range in Wyoming. This rate seems unlikely for several reasons:

- The rate results in a poor correlation with the eustatic high stands, which would be the time of fluvial deposition and surface stabilization
- It would mean an age of only 200 ka for the Puente Hills, an age not supported by recent work in the Coyote Hills (R. S. Yeats, personal communication), and
- It would place a 7 mm/yr slip rate onto the Whittier fault, a rate that exceeds the strain entering the LA Basin from the Elsinore fault (WGCEP, 1995).

The implications are that either the OSL ages are minimum ages, or both the accumulated soil chronosequence and the slip rate of the Whittier fault are incorrect. Soil ages reported herein are referenced to unpublished work and abstracts (Rockwell et al., 1988, 1992) but are deemed reliable because they are placed in context of numerous studies throughout southern California. In our experience, soil ages have large error bars, but they agree well with results of other types of dating in the Los Angeles basin. The soil chronosequence has been developed over the last

two decades principally using the marine terrace eustatic sequence for development age calibration. The soil ages determined for the San Joaquin Hills were well correlated with the coral ages measured for the same terrace (Grant et al, 1999). The Whittier fault's 1.1-1.4 mm/yr slip rate was measured by C-14 dating of channel deposits laterally displaced from a primary feeder channel, resulting in a minimum slip rate value (Gath dissertation, Chapter 2, in prep.). The rate of slip was determined from only one of at least two parallel fault strands, but because both faults had similar geomorphic expression, the slip rate was determined to be between 2-3 mm/yr. If there are additional faults carrying slip, they are not as well expressed in the landscape, and therefore would not increase this rate significantly.

Using OSL dates to correlate the Puente Hills terraces results in a 60 ka age for Qt3, and an implausibly high 6.7 mm/yr slip rate for the Whittier fault. Additional problems arise in that the terrace correlations are based on surface elevations and surface ages. The OSL sample age is based on sediment age. The sediment age is older than the geomorphic surface that has formed upon those sediments, meaning that surface age is even younger than the OSL age, and the uplift rate, and Whittier fault slip rate, would also need to be increased even more.

OSL age calculations are based on two factors: the sensitivity of the minerals to electron excitation, and the dose rate of that excitation due to natural, in-situ radiation. The initial efflorescence value is measured in the lab, and the mineral sensitivity is measured by artificially exposing the sample to a set dose rate. The in-situ dose rate is measured separately using a bulk sample collected in the sediments surrounding the sample location. The initial efflorescent value is then divided by the dose rate to arrive at the age of the sample. Two principal (and untestable) assumptions are that the electron excitation of the quartz atoms does not fade over time, and that the current dose rate has remained constant. If the dose rate of today is higher than the dose rate of the past, then the sample will yield a younger age. A change in dose rate could explain the unexpectedly young ages being returned by the OSL laboratory.

Other studies (projects by Earth Consultants International., Santa Ana, CA 2003-2006) using OSL, C-14, and soils in combination for age control have yielded similar lack of correlation, but only for ages exceeding 30 ka. In one instance, an 11.7 ka C-14 age on a large piece of detrital charcoal also returned a 12 ka OSL age from the surrounding fluvial sands. The error range for the OSL sample easily encompassed the age range for the charcoal sample. However, in another study involving OSL and soils, the OSL ages were consistently lower than the soil ages, by an average of 50% for terraces of approximately the same age as those from Santa Ana Canyon.

When deposited, the terrace sediments would have been within the active fluvial environment, probably fully saturated. They would have remained in this condition until left elevated by sea level fall and river entrenchment during the transition from interglacial to glacial conditions. The climatic shift from the glacial climate of 15-30 ka to the interglacial of today would involve large changes in the groundwater regime of the terraces. The climate was substantially wetter and colder 15-30 ka. Streams were entrenched, dropping local water tables accordingly. The colder and wetter conditions would have resulted in an increased unsaturated flow through the terrace sediments that would be quite different than the saturated conditions of deposition. Transition back to the warmer and dryer postglacial conditions of today would introduce another hydrologic change in the groundwater regime of the terrace sediments.

Mobility of radiogenic nuclides in groundwater might also affect the dose rate. The environment of deposition was very different than that in which they were sampled for this study, and neither environment is representative of the glacial intervals. Further complicating the OSL ages are the changes in sediment chemistry that result due to pedogenic mineral weathering and clay translocation. How radiogenic minerals migrate through, or are retained within, the terrace sediments throughout all these physical and temporal changes lies at the heart of the OSL dating accuracy. Agreement between OSL and C-14 ages in the most recent climatic cycle, and divergence from the prior cycle, is probably not random accident. We propose that OSL ages be viewed as a minimum ages if they span a glacial/interglacial eustatic cycle in the southern Los Angeles basin.

4.2 Basin Analysis

Preliminary analysis of basins in the Puente Hills (PH) and Santa Ana Mountains (SAM) was conducted by Gath et al. (2002) to estimate the ages of the basins and place constraints on the time since emergence of the PH and SAM. We have recalculated basin areas and developed new relationships between basin age and area. These relationships are still preliminary. See Gath et al., 2002 for methods.

4.2.1 Puente Hills Basin Analysis

As the Puente Hills are elevated, they are also eroded by running water. The independently determined ages of the streams (Gath, 1997; Gath et al., 2002; Gath June 2007 unpublished dissertation draft) provide constraints on the rate of drainage basin development. If there is a relationship between basin area and age, then that relationship can be applied to other geologically and climatically similar terranes to estimate age. Figure A shows fifteen primary drainage basins in the eastern Puente Hills that were selected for analysis. Only those drainage basins old enough to have experienced at least two climatic (glacial and interglacial) cycles were used in the analysis. The basins were drawn automatically using MapInfo software and USGS DEM data shown graphically in Figure A. The basins were all truncated at the Whittier fault because any basin enlargement downstream of the fault could not be correlated with those basins that actually terminate at the fault (i.e. all of the secondary basins). Although there are hundreds of smaller basins that are also offset by the Whittier fault, this analysis was limited to those basins that are old enough to have been through at least two complete glacial-interglacial climatic cycles to eliminate potentially significant variations in precipitation (and erosion) rates across those time periods. Additionally, the DEM data accuracy could begin to introduce non-quantifiable errors into the calculations at the smaller scale of these tertiary basins.

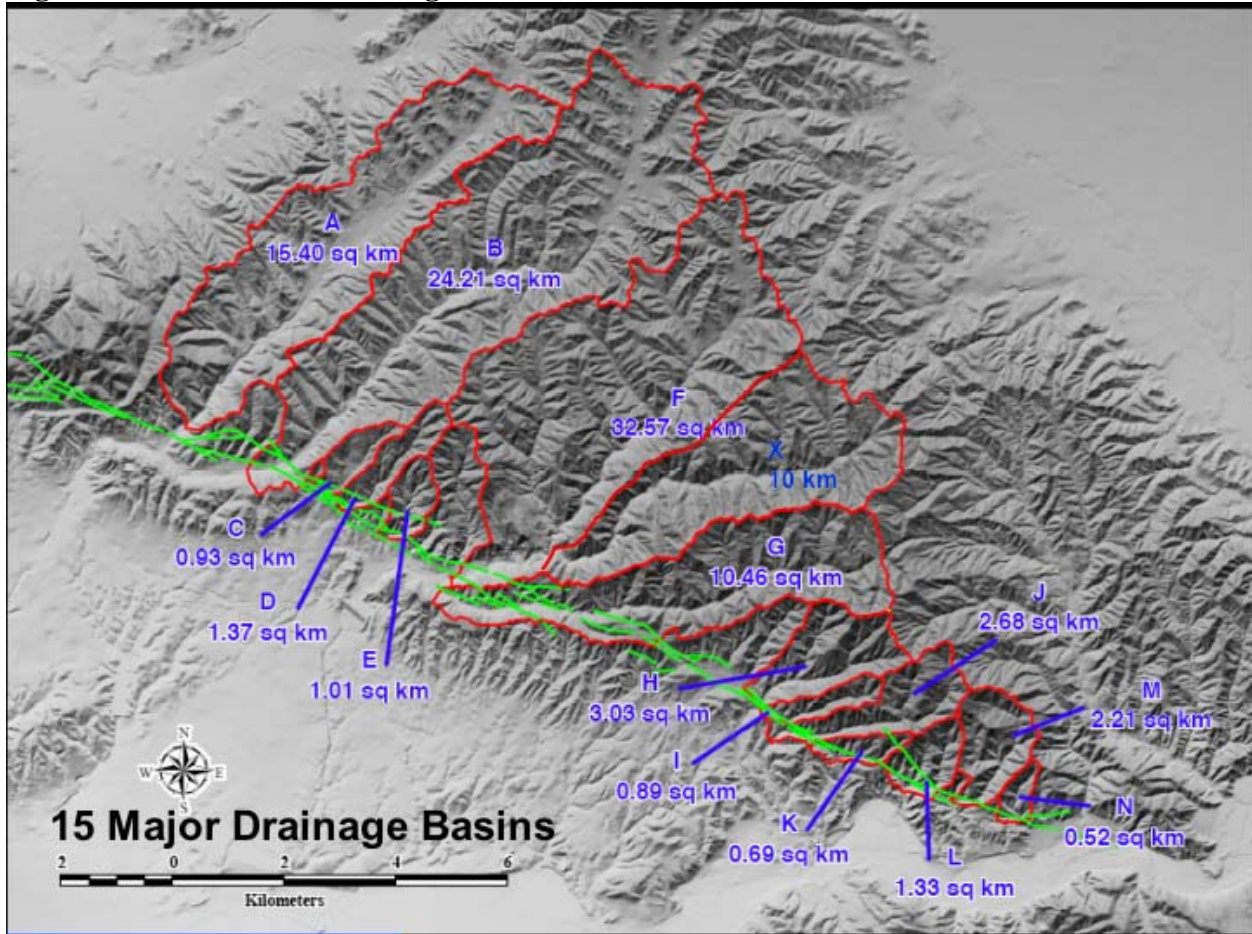
Soquel Canyon (basin X on Figure A) required more complex analysis. This large drainage basin has been captured by the Carbon Canyon drainage, and as such, was initially incorporated into analysis of the Carbon Canyon area (Gath et al., 2002). Its upstream drainage area is about 10 km², and its former outlet is a wind gap located 0.6 km east of the current Carbon Canyon outlet. In this analysis, Soquel Canyon is treated separately. Table A shows the calculated basin area and measured fault offsets of the 15 primary drainage basins in the eastern Puente Hills. The

basin ages were calculated assuming a 3 mm/yr slip rate for the Whittier fault. Figure B is a Plot of the Basin Area regressed against Basin Age (see Gath et al., 2002 for methods).

TABLE A

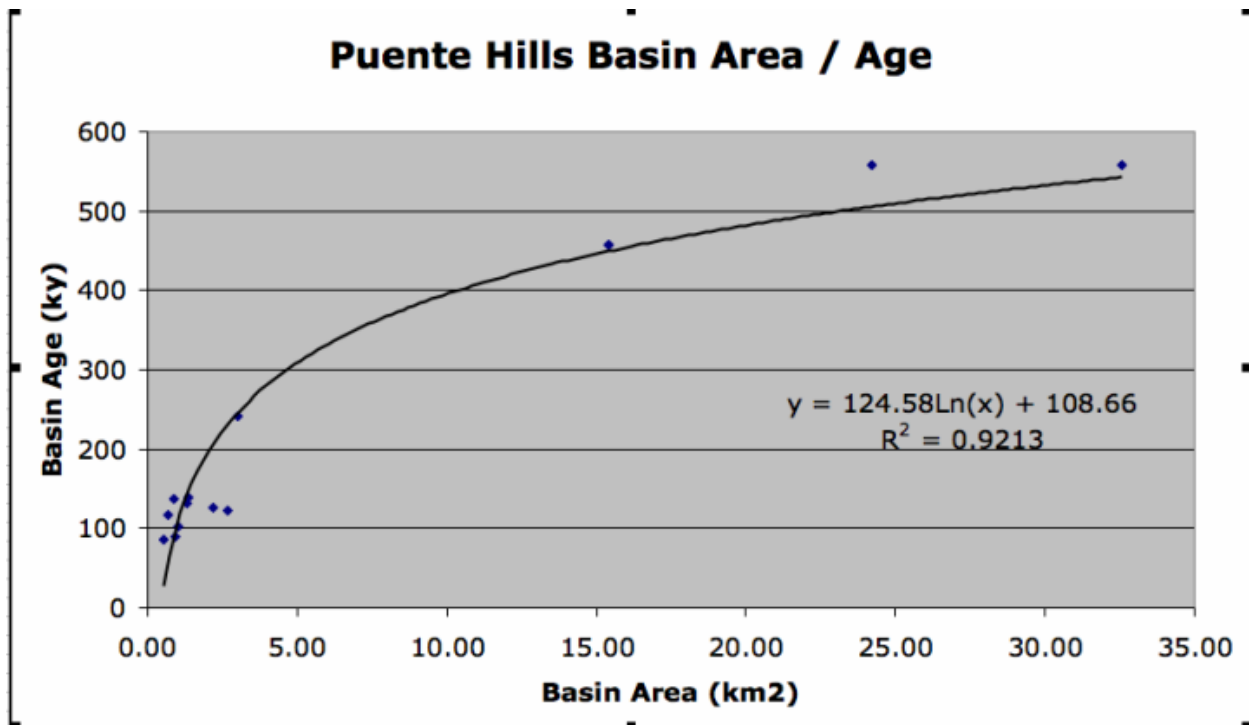
Map ID	Basin Name	Area km*2	Offset, km	Age, ka
A	Brea	15.40	1.37	157
B	Tonner	24.21	1.68	559
C	Olinda Landfill	0.93	0.27	90
D	Olinda a	1.37	0.42	140
E	Olinda b	1.01	0.31	102
F	Carbon	22.57	1.68	559
G	Telegraph	10.46	1.17	390
H	Travis Ranch	3.03	0.73	242
I	Yorba Linda	0.89	0.41	137
X	Soquel	10.00	1.21	403
J	Blue Mud	2.68	0.37	122
K	Lomas de Yorba	0.69	0.35	117
L	Box	1.33	0.40	132
M	Bee	2.21	0.38	127

Figure A – Puente Hills drainage basins and areas



Results, shown in Figure B, imply that the Puente Hills became emergent about 600 – 700 ka. The Puente Hills (PH) are seismically active and tectonically uplifted by the Puente Hills Blind Thrust fault (PHBTF). The rate of uplift, and consequently, the late Quaternary slip rate of the eastern part of the PHBTF, herein named the Santa Ana segment, can be constrained by ages of Quaternary stream terraces and strath surfaces in the Santa Ana River Canyon. The PH are cut by the 2-3 mm/yr right-lateral Whittier fault, itself capable of M6.7-7.2 earthquakes. The 7 mapped fill and strath terraces surfaces of the PH are cut by the Whittier fault with minimal vertical separation. OSL dating, soil age estimates, and correlation with sea level highstands constrains the PH uplift rate to 0.6-1.4 mm/yr based on OSL dates, and 0.2-0.8 mm/yr from other methods. The rates overlap in the range 0.6-0.8 mm/yr, and we propose that this is the most reliable estimate of uplift rate because it is based on multiple methods. An uplift rate of 0.6-0.8 mm/yr for the PH is also consistent with a 500 – 700 ka emergent age based on our geomorphic analysis of PH drainage basin development. Using a 30° dip angle produces a slip rate on the Santa Ana segment of the PHBTF of 1.2-1.6 mm/yr.

Figure B



4.2.2 Santa Ana Mountains Basin Analysis

Preliminary tectonic geomorphic analysis of the Santa Ana Mountains (SAM) suggests that they too are being uplifted and are probably seismically active (Gath et al., 2002). Shorelines preserved on the lower foothills of Peralta and Loma Ridges were correlated to eustatic sea levels for age estimations. Mapping and dating of terraces in the Santiago Creek drainage (Figures C and D), and the older marine terraces indicates that the SAM are uplifting at 0.3-0.8 mm/yr, probably due to a blind thrust associated with partial termination of the Elsinore fault. This rate is confirmed by the 0.4-0.5 mm/yr rate obtained from the 80-120 ka emergent terrace on the western nose of Burrell Ridge, uplifted by the Peralta Hills fault (Grant et al., 2006). At these rates, the SAM became emergent ~ 2 – 4 Ma.

Figure C

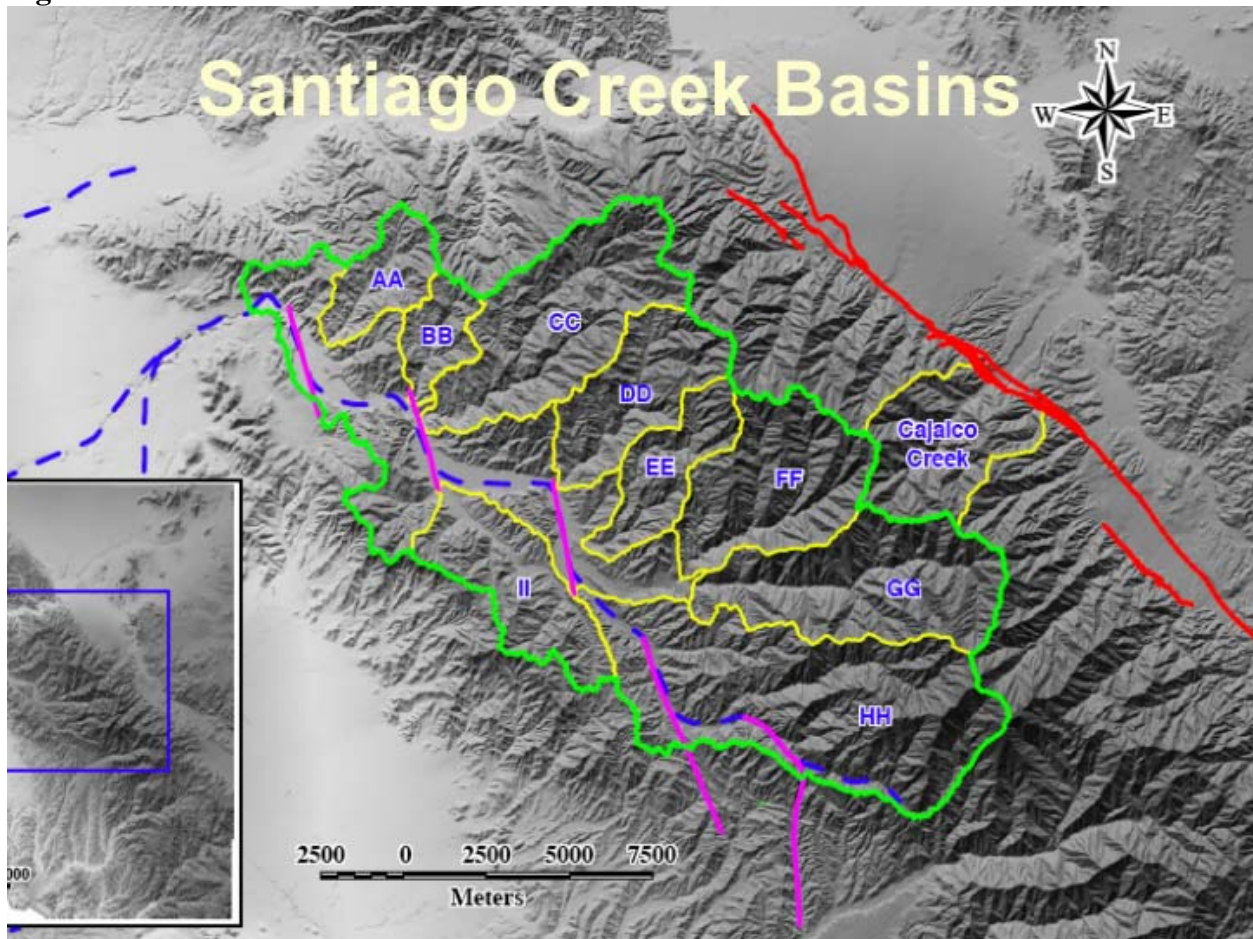
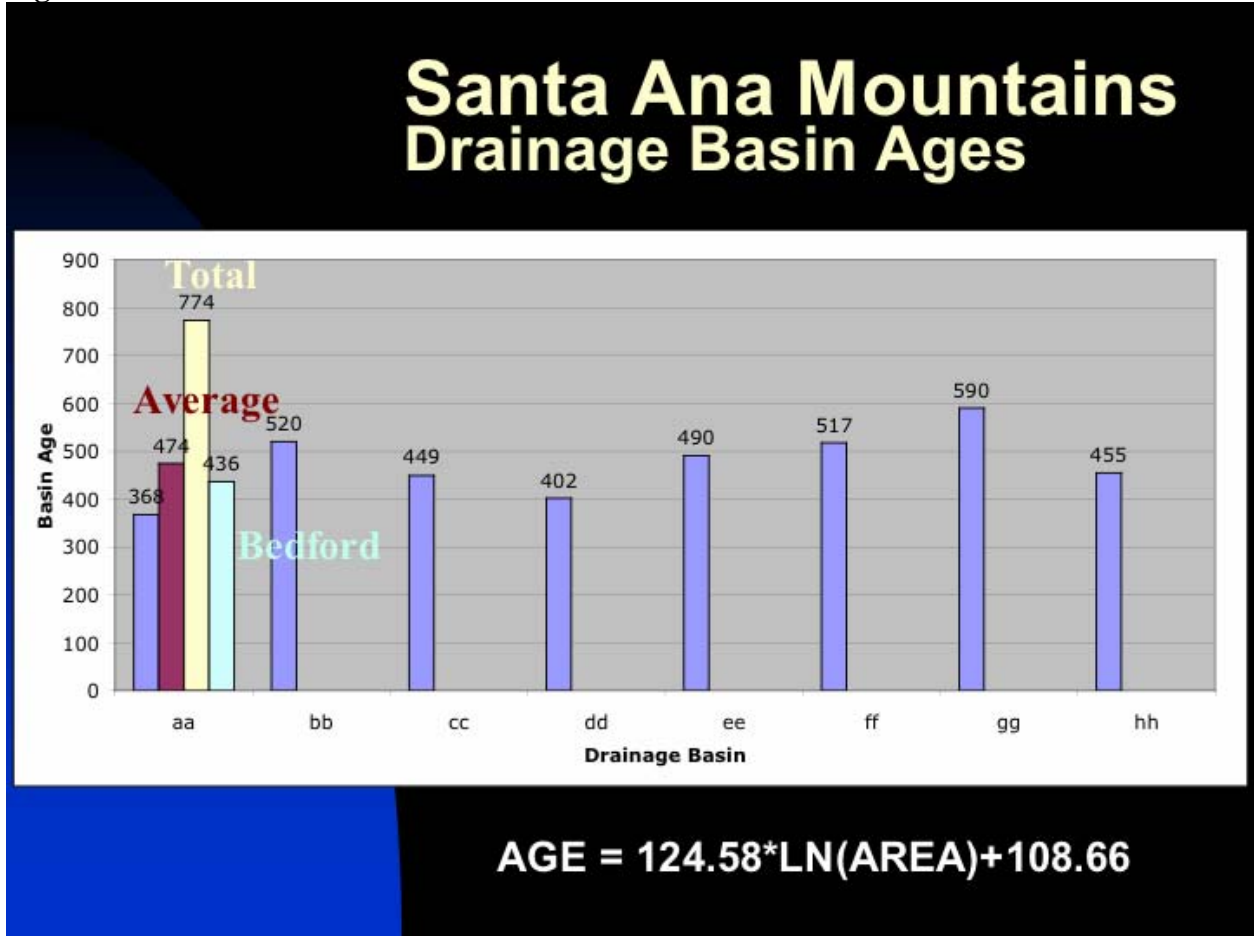


Figure D



4.3 Summary and Neotectonic model

Indentor tectonics: A new model to describe Quaternary geomorphic development and seismic hazards of southeastern Los Angeles basin, Orange County, California

This section is modified from Chapter 5 of Gath's draft dissertation (June 2007 version) describing a neotectonic model for the geomorphic development of Orange County, including the San Joaquin Hills (SJH), Santa Ana Mountains (SAM), Loma Ridge (LM), and Puente Hills (PH). In this model, the SAM became emergent approximately 2-4 Ma at a rate of 0.2-0.7 mm/yr. LR formed 2.5 Ma and blocked northern SAM drainages from flowing directly to the ocean. LR is interpreted as a southwest-vergent structure, obliquely accommodating north-south crustal shortening when the southern Newport-Inglewood fault (NIF) terminated into a right-stepping horsetail splay (consisting of the Cristianitos, Mission Viejo and Dana Cove faults). In the mid-Quaternary, the NIF stepped westward onto the Northern NIF branch, resulting in the compressional step that formed the SJH, a north-vergent, anticlinally deformed structure, bounded on the east by the Dana Cove fault, driven by strain partitioning off of the NIF, emergent less than 1 Ma, and uplifting at 0.25 mm/yr since 122 ka. At 200-300 ka, the NIF straightened into the LA Basin along the Southern NIF branch, producing uplift of Signal Hill, eliminating the source of compressive strain for the LR anticline.

The PH became emergent 500-700 ka at 0.8 mm/yr, by uplift along the PH blind thrust fault (PHBTF). The PHBTF is accommodating N-S compressional strain, while the right-lateral Whittier fault is accommodating 2-3 mm/yr of NW vergent lateral strain of the Elsinore fault's (EF) 5-6 mm/yr slip. The Coyote Hills are an en-echelon series of hanging wall folds similar to LR, caused by thrusting the SAM block into Santa Ana River (SAR) sediments, using the PHBTF as a decollement. The Chino fault, a right-lateral extension of the EF, accommodates 1-2 mm/yr motion, which results in an EF strain surplus of 1-3 mm/yr for uplift of the SAM. The Peralta Hills fault, an EF backthrust, deflects the SAR 3 km westward by uplift of LR. The regional deformation is driven by the SAM moving northwest as an "indentor" and compressing the soft sedimentary fill in the eastern Los Angeles basin. The indentor is being driven northwestward at a rate of approximately 6 mm/yr along the EF. Due to inertia and pinning by the NIF and SJH thrust, the overlapping sedimentary deposits on the southwestern side of the SAM are being underthrust and deformed by movement of the SAM batholith. Deformation is accommodated by compressional folding of LR, and a left-lateral shear zone along Santiago Creek and the SAM foothills. Shearing has caused 3 km deflections of Santiago Creek due to drag and block rotation. The southern extent of the shear zone is uncertain, but the total displacement along it must be in the range of 12-15 km based on a Holtz Shale piercing line, and the total displacement of a unique diatomaceous shale unit across both sides of the SAM. The seismic hazard implications of this model are uncertain.

According to this model, dextral strain at a rate of 6 mm/yr along the EF should be balanced by sinistral shearing (along the 4-S Ranch and other faults) and by block rotations along the southwestern side of the SAM indentor. Block rotations are likely accommodated through reactivation of proximal Miocene normal faults (Mission Viejo, Cristianitos, Dana Point, Bee Canyon, El Modena, and unnamed N-S trending faults) that formed during Borderlands extension. The lateral shearing would be most disseminated at the northern end of the indentor,

becoming increasingly consolidated and formed southward where the total slip increases. The best expression of this shear zone is the 4-S Ranch fault near the intersection of El Toro Road and Live Oak Canyon. At the northern tip of the indenter, the sedimentary strata are being underthrust and deformed onto the more rigid batholithic rocks. This results in northward tilting and extensive faulting and folding of the units. The Holtz Shale appears to be accommodating much of the basal thrusting, as it is repeated at least once along a SW-SE transect across the nose of the northern SAM. Repetition of this section is best explained by imbricate thrusting.

Rates of deformation constrained by geomorphic analysis and dating of Quaternary terraces, as described in this report, suggest that significant tectonic deformation is ongoing. This indenter neotectonic model implies that seismic hazard in Orange County is higher than previously estimated because there is a previously unrecognized zone of distributed deformation in southeastern Orange County along the foothills of the Santa Ana Mountains.

REFERENCES

- Adamiec, G., and Aitken, M., 1998. Dose-rate conversion factors: update: *Ancient TL*, 16, 37-50.
- Aitken, M.J., 1998. *An introduction to optical dating*. Oxford University Press, Oxford.
- Bortolot, V.J., 1997. Improved OSL excitation with fiberoptics and focused lamps. *Radiation Measurements*, 27, 101-106.
- Bryant, M.E. & Fife, D.L. (1992). The Peralta Hills fault, a Transverse Ranges structure in the northern Peninsula Ranges, southern California. in Fife, D.L. & Minch, J.A. (eds), *Geology and Mineral Wealth of the California Transverse Ranges*. South Coast Geological Society, Santa Ana, California, p. 403-409.
- Bullard, T.F. & Lettis, W.R. (1993). Quaternary fold deformation associated with blind thrust faulting, Los Angeles basin, California. *Journal of Geophysical Research*, 98 (B5), 8349-8369.
- Cox, R.T. (1994). Analysis of drainage basin symmetry as a rapid technique to identify areas of possible Quaternary tilt-block tectonics: An example from the Mississippi Embayment. *Geological Society of America Bulletin*, 106, 571-581.
- Crone, A.J., Machette, M.N., Bradley, L-A. and Mahan, S.A. 1997. Late Quaternary surface faulting on the Cheraw Fault, Southeastern Colorado. *Geologic Investigations Map*, USGS Map I-2591.
- Crouch, J.K. and Suppe, J., 1993, Late Cenozoic tectonic evolution of the Los Angeles basin and inner California borderland: a model for core complex-like crustal extension: *Geological Society of America Bulletin*, v. 105, p. 1415-1434.
- Davis, T.L., Namson, J., and Yerkes, R.F., 1989, A cross section of the Los Angeles area: seismically active fold and thrust belt, the 1987 Whittier Narrows earthquake, and earthquake hazard; *Journal of Geophysical Research*, v. 94, n. B7, p. 9644-9664.
- Dolan, J.F., Christofferson, S.A., and Shaw, J.H., 2003, Recognition of paleoearthquakes on the Puente Hills blind thrust fault, California; *Science*, v. 300, p. 115-118.
- Durham, D.L. & Yerkes, R.F. (1964). Geology and oil resources of the eastern Puente Hills area, southern California. *U.S. Geological Survey Professional Paper 420-B*, 62 p.
- Gath, E.M. (1997). Tectonic geomorphology of the eastern Los Angeles Basin. *USGS Final Technical Report, NEHRP Contract No. 1434-95-G-2526*, 13 p., 1 plate, 6 figures, 6 tables.
- Gath, E.M., Gonzalez, T., & Rockwell, T.K. (1992). Evaluation of the late Quaternary rate of slip, Whittier fault, southern California. *USGS Final Technical Report, NEHRP Contract No. 14-08-0001-G1696*, 24 p., numerous plates.
- Gath, E. M., Runnerstrom, E. E. and L. B. Grant (PI) (2002). Active deformation and earthquake potential of the southern Los Angeles basin, Orange County, California. U.S. Geological Survey National Earthquake Hazard Reduction Program, Final Technical Report, Award Number 01HQGR0117.
- Gath, E. M. and Grant, L. B. (2002). Is the Elsinore fault responsible for the uplift of the Santa Ana Mountains, Orange County, California? *GSA Abstracts with Programs*, v. 34, no. 5, April, p. A-87, 2002.
- Gath, E. M. and L. B. Grant (2004). Learning from Northridge: A progress report on the active faults of Orange County, *Seism. Res. Ltrrs.*, 75 (2), March/April, p. 260.

- Gath, E., L. Grant and E. Runnerstrom (2003a). Using strike-slip offsets for temporal control of the development of a Quaternary drainage network in southern California, (abs) Program with Abstracts, Association of Engineering Geologists, 2003 Annual Meeting, AEG NEWS, v. 46, p. 56.
- Gath, E., L. Grant, and L. Owen (2003b). Temporal controls on vertical motion rates for the Santa Ana Mountains and Puente Hills, Orange County, California, Proceedings and Abstracts, v. XIII, SCEC Annual Meeting, p.88.
- Grant, L. B., J. T. Waggoner, C. von Stein and T. Rockwell (1997). Paleoseismicity of the North Branch of the Newport-Inglewood Fault Zone in Huntington Beach, California, from Cone Penetrometer Test Data. *Bulletin Seismological Society of America*, v. 87, no. 2, 277 - 293.
- Grant, L.B., Mueller, K.J., Gath, E.M., Cheng, H., Edwards, R.L., Munro, R., & Kennedy, G.L. (1999). Late Quaternary uplift and earthquake potential of the San Joaquin Hills, southern Los Angeles basin, California. *Geology*, 27, 1031-1034.
- Grant, L.B., Mueller, K.L., Gath, E.M., & Munro, R. (2000). Late Quaternary uplift and earthquake potential of the San Joaquin Hills, southern Los Angeles basin, California – REPLY, *Geology*, 28, (4), 384.
- Grant, L.B., Ballenger, L.J., & Runnerstrom, E.E. (2002). Evidence of a large earthquake and coastal uplift of the San Joaquin Hills, southern Los Angeles basin California, since 1635 A.D. *Bulletin of Seismological Society of America*, 92, (2), 590-599.
- Grant, L. B., and Rockwell, T. K.(2002). A Northward propagating earthquake sequence in coastal southern California? *Seismological Research Letters*, v. 73, no. 4, p.461-469, 2002.
- Harden (1982)
- Hauksson, E., 1990, Earthquakes, faulting, and stress in the Los Angeles basin; *Journal of Geophysical Research*, v. 95, n. B10, p. 15,365-15,394.
- Hauksson, E. and Jones, L.M., 1989, The 1987 Whittier Narrows earthquake sequence in Los Angeles, southern California: seismological and tectonic analysis; *Journal of Geophysical Research*, v. 94, n. B7, p. 9569-9589.
- Hauksson and Gross, 1991
- Heath, E.G., Jensen, D.E., & Lukesh, D.W. (1982). Style and age of deformation on the Chino fault: in Cooper, J.D. (ed.), *Neotectonics in southern California: Geological Society of America Cordilleran Section, Field Trip Guidebook*, 123-134.
- Hull, A.G. & Nicholason, C. (1992). Seismotectonics of the northern Elsinore fault zone, southern California. *Bulletin of the Seismological Society of America*, 82, (2), 800-818.
- Kent, G.M., Babcock, J.M., Driscoll, N.W., Harding, A.J., Dingler, J.A., Seitz, G.G., Gardner, J.V., Mayer, L.A., Goldman, C.R., Heyvaert, A.C., Richards, R.C., Karlin, R., Morgan, C.W., Gayes, P.T. and Owen, L.A., 2005. A 60 k.y. record of extension across the western boundary of the Basin and Range province: estimate slip rates from offset shoeline terraces and a catastrophic slide beneath Lake Tahoe. *Geology*, in press.
- Kirby, E. & Whipple, K. (2001). Quantifying differential rock-uplift rates via stream profile analysis. *Geology*, 29, 415-418.
- Lamar, D.L. & Rockwell, T.K. (1986). An overview of the tectonics of the Elsinore fault zone; in Ehlig, P.L. (ed.), *Neotectonics and faulting in southern California, Geological Society of America Cordilleran Section, Field Trip Guidebook*, 149-158.
- Lee, J., Spencer, J.Q. and Owen, L.A., 2001. Holocene slip rates along the Owens Valley fault, California: implications for the recent evolution of the Eastern California Shear Zone. *Geology*, 29, 819–822.
- Machette, M.N., Personius, S.F. and Nelson, A.R., 1992. The Wasatch Fault Zone, USA. *Annales Tectonicae*, 6, 5-39, 5-39.
- Mejdahl, V., 1979. Thermoluminescence dating: Beta attenuation in quartz grains. *Archaeometry*, 21, 61-73.
- Merritts, D.J., Vincent, K.R., & Wohl, E.E. (1994). Long river profiles, tectonism, and eustasy: A guide to interpreting fluvial terraces. *Journal of Geophysical Research*, 99, (B7), 14,031-14,050.
- Montgomery, D.R. (1994). Valley incision and the uplift of mountain peaks. *Journal of Geophysical Research*, 99, 13,913-13,921.
- Morton, P.K. & Miller, R.V. (1981). Geologic map of Orange County, California showing locations of mines and mineral deposits. *California Division of Mines and Geology Bulletin* 204, 1:48,000.
- Murray, A. S., and Wintle, A. G., 2000. Luminescence dating of quartz using an improved single-aliquot regenerative-dose protocol. *Radiation Measurements*, 32, 57-73.
- Nicol, A., Alloway, B., & Tonkin, P. (1994). Rates of deformation, uplift, and landscape development associated with active folding in the Waipara area of North Canterbury, New Zealand. *Tectonics*, 13, 1327-1344.
- Ohmori, H. (1993). Changes in the hypsometric curve through mountain building resulting from concurrent tectonics and denudation. *Geomorphology*, 8, 263-277.

- Owen, L.A., Cunningham, W.D., Richards, B., Rhodes, E.J., Windley, B.F., Dornjamjaa, D., Badamgarav, J., 1999. Timing of formation of forebergs in the northeastern Gobi Altai, Mongolia: implications for estimating mountain uplift rates and earthquake recurrence intervals. *Journal of the Geological Society*, 156, 3, 457-464. Erratum: *Journal of the Geological Society*, 156, Contents xii.
- Pazzaglia, F.J., Gardner, T.W., & Merritts, D.J. (1998). Bedrock fluvial incision and longitudinal profile development over geologic time scales determined by fluvial terraces: Rivers over Rock - Fluvial Processes in Bedrock Channels. American Geophysical Union, Geophysical Monograph, 107, 207-235.
- Personius, S.F., 1993, Age and origin of fluvial terraces in the central Coast Range, western Oregon; U.S. Geological Survey Bulletin 2038, 56 p.
- Petersen, M.D. and Wesnousky, S.G., 1994, Fault slip rates and earthquake histories for active faults in southern California; *Seismological Society of America Bulletin*, v. 84, p. 1608-1649.
- Peterson, M.D., Bryant, W.A., Cramer, C.H., Cao, T., Reichle, M.S., Frankel, A.D., Lienkaemper, J.J., McCrory, P.A., Schwartz, D.P., 1996, Probabilistic seismic hazard map for California; California Division of Mines and Geology, OFR 96-08 and USGS OFR 96-706, 1 plate.
- Ponti, D.J., Lajoie, K.R., Conlan, L.M., and McKereghan, P.F., 1986, Episodic Quaternary marine sedimentation in the southwestern Los Angeles Basin (abs); *Geological Society of America Abstracts with Programs*, v. 18, n. 2, p. 171.
- Ponti, D.J., Lajoie, K.R., Powell II, C.L., 1991, Upper Pleistocene marine terraces in San Pedro, southwestern Los Angeles basin, California: Implications for aminostratigraphy and coastal uplift; *Geological Society of America Abstracts with Programs*, v. 23, n. 2, p. 89.
- Prescott, J. R., and Hutton, J. T., 1994. Cosmic ray contributions to dose rates for luminescence and ESR dating: Large depths and long-term time variations. *Radiation Measurements*, 23, 497-500.
- Rockwell, T.K., Gath, E.M., & Cook, K.D. (1988). Sense and rate of slip on the Whittier fault zone near Yorba Linda, California (abs.). Abstracts with Programs, Cordilleran Section, Geological Society of America, 20, (3), 224.
- Rockwell, T.K., Gath, E.M., & Gonzalez, T. (1992). Sense and rate of slip on the Whittier fault zone, eastern Los Angeles basin, California. in Stout, M.L. (ed), Proceedings of the 35th Annual Meeting, Association of Engineering Geologists, 679.
- Rockwell, T.K., Lindvall, S., Herzberg, M., Murbach, D., Dawsaon, T. and Berger, G., 2000. Paleoseismology of the Johnson Valley, Kicjapoo, and Homestead Valley Faults: clustering of earthquakes in the Eastern California Shear Zone. *Bulletin of the Seismological Society of America*, 90, 5, 1200-1236.
- Rosenbloom, N.A., & Anderson, R.S. (1994). Hillslope and channel evolution in a marine terraced landscape, Santa Cruz, California. *Journal of Geophysical Research*, 99, 14,013-14,029.
- Schoellhamer, J.E., Vedder, J.G., Yerkes, R.F., & Kinney, D.M. (1981). Geology of the northern Santa Ana Mountains, California. U.S. Geological Survey Professional Paper 420-D, 109 p.
- Schumm, S.A. (1986). Alluvial river response to active tectonics, in *Studies in National Research Council (eds), Active Tectonics*. National Academy Press, Studies in Geophysics, Washington, D.C., 80-94.
- Schumm, S.A., Mosley, M.P., & Weaver, W.E. (1987). *Experimental fluvial geomorphology*: John Wiley & Sons, New York, 413 p.
- Shaw, J.H. & Shearer, P.M. (1999). An elusive blind-thrust fault beneath metropolitan Los Angeles. *Science*, 283, 1516-1518.
- Shaw et al. (2002).
- Walls, C., and Gath, E.M., 2001, Tectonic geomorphology and Holocene surface rupture on the Chino fault: Southern California Earthquake Center Annual Meeting, proceedings and Abstracts, p. 118.
- Washburn, Z., Arrowsmith, J.R., Forman, S.L., Cowgill, E., Wang Xiaofeng, Zhang Yueqiao and Chen Zhengle, 2001. Late Holocene earthquake history of the central Altyn Tagh fault, China. *Geology*, 29, 11, 1051-1054.
- Wesnousky, S.G., Barron, A.D., Briggs, R.W., Caskey, S.J., Kumar, S. and Owen, L.A., 2005. Paleoseismic transect across the northern Great Basin, USA. *Journal of Geophysical Research*, in press.
- Whitney, R.A. & Seymour, D.C. (1992). Active strike-slip faulting within the Peralta Hills anticline, Orange County, California—a Transverse Range-Peninsula Range boundary. American Association of Petroleum Geologists, 76, 432.
- Wohl, E.E. (1998). Bedrock channel morphology in relation to erosional processes; Rivers over Rock: Fluvial Processes in Bedrock Channels. American Geophysical Union, Geophysical Monograph, 107, 133-151.
- Working Group on California Earthquake Probabilities (WGCEP) (1995). Seismic hazards in southern California: probable earthquakes, 1994 to 2024; *Seismological Society of America Bulletin*, v. 85, p. 379-439.

Yerkes, R.F. (1972). Geology and oil resources of the western Puente Hills area, southern California. U.S. Geological Survey Professional Paper 420-C, 63 p.

Table 1. Summary of OSL dating results from quartz extracted from sediment matrices: sample locations, radioisotope concentrations, moisture contents, total dose-rates, D_E estimates and optical ages

Sample #	Particle size (μm)	Location (N/E)	a.s.l. (m)	Depth (cm)	U ^a (ppm)	Th ^a (ppm)	K ^a (%)	Rb ^a (ppm)	$W_{in-situ}$ ^b (%)	Cosmic ^c (mGya ⁻¹)	Dose-rate ^d (mGya ⁻¹)	N ^{e,f}	Mean D_E ^g (Gy)	Age ^h (ka)
EG#1	90-125	33.78°/ 117.84°	30	310	1.54	5.89	1.70	59.30	2.4	0.15±0.01	2.44±0.16	10 (24)	10.2±5.7	4.2±0.8 4.6±0.9
EG#2	90-125	33.78°/ 117.84°	30	390	2.14	9.25	1.73	57.50	2.3	0.13±0.01	2.82±0.18	8 (8)	18.0±8	6.3±1.1 7.1±1.2
LG1	90-125	33.778°/ 117.707°	261	600	2.07	9.06	2.4	73.4	7.3	0.10403	3.18±0.21	19	195.13±65.76	61.4±6.9 64.3±6.4
LG2	90-125	33.778°/ 117.707°	261	300	1.45	6.23	2.1	64.3	4.0	0.14415	2.69±0.18	8 (9)	157.30±41.54	58.5±7.3 62.1±7.1
LG3	90-125	33.769°/ 117.714°	245	50	2.00	7.58	2.0	50.1	9.1	0.19273	2.81±0.18	15 (42)	144.90±37.92	51.5±5.4 53.7±4.9
LG4	90-125	33.838°/ 117.845°	92	245	3.38	12.30	2.1	83.0	12.1	0.14962	3.51±0.21	10	(264.66±95.63) ⁱ >>300	(75.4±13.5) ⁱ >75 > 79.8±10.2
LG6	90-125	33.526°/ 117.450°	122	70	0.86	8.70	3.4	106.0	2.2	0.18659	3.82±0.27	11	121.75±49.32	31.9±4.8 33.3±4.7
LG7	90-125	33.778°/ 117.709°	130	500	2.47	6.32	1.9	55.0	6.5	0.11335	2.69±0.17	18	102.24±28.32	38.0±3.9 40.0±3.6
LG8	90-125	33.88°/ 117.69°	134	1000	2.48	12.40	2.23	94.30	1.6	0.07±0.01	3.51±0.22	19 (43)	102.9±28.6	29.3±3.0 32.6±2.9
LG9	90-125	33.88°/ 117.71°	144	200	2.25	8.76	1.61	68.80	6.2	0.17±0.02	2.71±0.16	30 (41)	63.6±7.5	23.5±1.9 25.6±1.6
LG11	90-125	33.87°/ 117.76°	131	150	2.68	8.55	1.59	67.70	9.4	0.18±0.02	2.69±0.16	9 (16)	121.2±35.7	45.0±5.6 47.5±5.4
LG12	90-125	33.81°/ 117.80°	109	400	1.52	5.31	1.92	68.00	5.9	0.13±0.01	2.56±0.17	19 (36)	136.5±40.0	53.3±5.7 58.6±5.5

^aElemental concentrations from NAA of whole sediment measured at USGS Nuclear Reactor in Denver. Uncertainty taken as ±10%.

^bEstimated fractional water content from whole sediment (Aitken, 1998).

^cEstimated contribution to dose-rate from cosmic rays calculated according to Prescott and Hutton (1994). Uncertainty taken as ±10%.

^dTotal dose-rate from beta, gamma and cosmic components. Beta attenuation factors for U, Th and K compositions incorporating grain size factors from Mejdahl (1979). Beta attenuation factor for Rb arbitrarily taken as 0.75 (cf. Adamiec and Aitken, 1998). Factors to convert elemental concentrations to beta and gamma dose-rates from Adamiec and Aitken (1998) and beta and gamma components attenuated for moisture content.

^eNumber of replicated D_E estimates used to calculate mean D_E . These are based on recuperation of < 10%.

^fThe number of samples used to determine the age. The total number of discs examined are shown in parenthesis.

^gMean equivalent dose (D_E) determined from replicated single-aliquot regenerative-dose (SAR; Murray and Wintle, 2000) runs. Errors are 1-sigma standard errors (ie. $\sigma_{n-1}/n^{1/2}$) incorporating error from beta source estimated at about ±5%.

^hAge in bold based on estimated water content of 15±5%, averaged through the life of the deposit. Age in regular type based on a 10±5% water content.

ⁱAge based on minimum D_E value.

TABLE 2 – Terrace elevations and sample locations

Sample#	Sample Name	Location (N/E)	Terrace	Sample Elevation (feet/meters)	Terrace Surface Elevation (feet/meters)	Base level Elevation (feet/meters)	Terrace height above base level (m)
LG1	Irvine Lake	33.778° 117.707°	Qt2	840 / 256	860 / 262	800 / 244	18
LG2	Irvine Lake	33.778° 117.707°	Qt2	840 / 256	860 / 262	800 / 244	18
LG3	Irvine Lake Campground	33.769° 117.714°	Qt2	855 / 261	860 / 262	800 / 244	18
LG4	Burrell Point	33.838° 117.845°	Qt1 or Qt3?	370 / 113	380 / 116	200 / 61	55
LG5	B.P. Block destroyed	33.838° 117.845°	Qt1 or Qt3?	370 / 113	380 / 116	200 / 61	55
LG6	Yorba Linda Estancia RR	33.526° 117.450°	Qt1	400 / 123	475 / 145	325 / 99	46
LG7	Lomas De Yorba West RR	33.778° 117.709°	Qt2	450 / 137	500 / 152	390 / 119	33
LG8	Lomas De Yorba East RR	33.88° 117.69°	Qt1	425 / 130	500 / 152	380 / 116	36
LG9	Lomas De Yorba House Park	33.88° 117.71°	Qt1	415 / 126	425 / 130	380 / 116	14
LG10	91 Fwy destroyed	33.87° 117.76°		433 / 132	440 / 134	315 / 96	38
LG11	Above 91 Freeway	33.87° 117.76°	Qt2	435 / 133	440 / 134	315 / 96	38
LG12	Santiago Rd Quarry	33.81° 117.80°	Qt1	370 / 113	440 / 134	330 / 101	33
LG13	S.R. Quarry Lost	33.49° 117.48°		360 / 110	440 / 134	330 / 101	33
LG14	Baker Cyn Lost	33.76° 117.68°		960 / 293	1000 / 305	920 / 280	25
EG1	22 Freeway Cut	33.78° 117.84°	Qal	190 / 58	205 / 62	190 / 58	4
EG2	22 Freeway Cut	33.78° 117.84°	Qal	185 / 56	205 / 62	190 / 58	4

Table 3 – Age of Fill Terraces in Santa Ana River Canyon, Puente Hills

Fill Terrace #	Terrace Height (m)	Preferred Age (ka)	Age Estimate (sea level substage correlation)	Age Estimate (soils)	OSL Age (see Table 1)	Geomorphic Position
Qa1	0	0	0	0	N/a	Modern river
Qt0	-24	30	30 ka (3a)	N/a	N/a	Buried terrace
Qt1		60	60 – 80 ka (3c, 5a)	40 ka	33.3±4.7 ka [LG-6] 32.6±2.9ka [LG-8] 25.6±1.6 ka [LG-9]	Cut and filled into toe of Qt2 (i.e. younger than Qt2)
Qt2		80	80 -120ka (5a, 5e)	80 ka	40.0±3.6 ka [LG-7] 47.5±5.4 ka [LG-11]	Fan deposits graded to Santa Ana River
Qt3		120	120 - 210 ka (5e, 7)	140 ± 70 ka		Incised into by streams offset 400 m by Whittier Fault; implies age is 133-200 ka
Qt4		≥ 210	≥ 210 ka (7+)	> 200 ka	N/a	Remnants, all north of WF

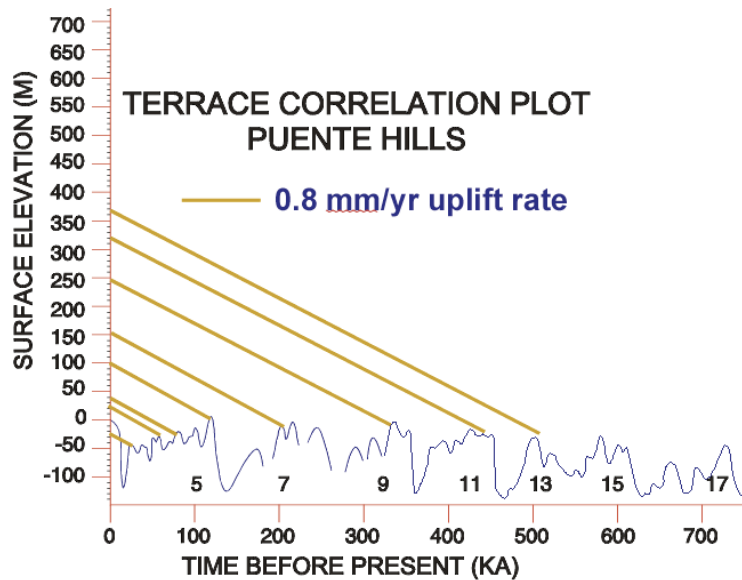


Figure 15: Correlation plot of Santa Ana Canyon terrace surfaces and the eustatic sea level curve using a constant 0.8 mm/yr uplift rate.

Table 4 – Age of Fill Terraces along Santiago Creek, Santa Ana Mountains

Fill Terrace #	Terrace Height (m)	Preferred Age (ka)	Age Estimate (sea level substage correlation)	OSL Age* (see Table 1)	Geomorphic Position
Qal	0	0	0	4.2±0.8 ka [EG-1] 6.3±1.1 ka [EG-2]	Holocene
Qt1		60	30 – 60 ka (3a, 3c)	58.6±5.5ka [LG-12]	
Qt2	18	80	60 – 80 ka (3c, 5a)	64.3±6.4 ka [LG-1] 62.1±7.1 ka [LG-2] 53.7±4.9 ka [LG-3]	
Qt3		120	105 - 120 ka (5c, 5e)	N/a	
Qt4		≥ 210	≥ 210 ka	N/a	

* For Holocene samples, OSL ages are based on 10 ± 5 % water content. Other sample ages are based on estimated 15 ± 5 % water content.

TABLE 5 Maximum and preferred uplift rates from minimum (OSL) ages and preferred ages. Santa Ana Mountains and Foothills values in italics. See Table 2 for sample and terrace surface elevations.

Sample#	Sample Name	Terrace	Terrace height above base level (m)	OSL age (minimum) (ka)	Uplift rate from OSL (m/ka)	Preferred age (ka) (Table 3, 4)	Preferred uplift rate (meters/ka)
<i>LG1</i>	<i>Irvine Lake</i>	<i>Qt2 / Santiago</i>	<i>18</i>	<i>64.3±6.4</i>	<i>0.28</i>	<i>80</i>	<i>0.225</i>
<i>LG2</i>	<i>Irvine Lake</i>	<i>Qt2 / Santiago</i>	<i>18</i>	<i>62.1±7.1</i>	<i>0.29</i>	<i>80</i>	<i>0.225</i>
<i>LG3</i>	<i>Irvine Lake Campground</i>	<i>Qt2 / Santiago</i>	<i>18</i>	<i>53.7±4.9</i>	<i>0.34</i>	<i>80</i>	<i>0.225</i>
<i>LG4</i>	<i>Burrell Point</i>	<i>Qt3 / SAR</i>	<i>55</i>	<i>> 79.8±10.2</i>	<i>< 0.69</i>	<i>120</i>	<i>0.46</i>
<i>LG5</i>	<i>Burrell Point [Block]</i>	<i>Qt3 / SAR</i>	<i>55</i>	<i>destroyed</i>	<i>--</i>	<i>--</i>	<i>--</i>
LG6	Yorba Linda Estancia RR	Qt1 / SAR	46	33.3±4.7	1.38	60	0.77
LG7	Lomas De Yorba West RR	Qt2 / SAR	33	40.0±3.6	0.82	80	0.41
LG8	Lomas DeYorba East RR	Qt1 / SAR	36	32.6±2.9	1.10	60	0.60
LG9	Lomas De Yorba House Park	Qt1 / SAR	14	25.6±1.6	0.55	60	0.23
LG10	Above 91 Freeway	Qt2 / SAR	38	destroyed	--	--	--
LG11	Above 91 Freeway	Qt2 / SAR	38	47.5±5.4	0.80	80	0.48
<i>LG12</i>	<i>Santiago Rd Quarry</i>	<i>Qt1 / Santiago</i>	<i>33</i>	<i>58.6±5.5</i>	<i>0.56</i>	<i>60</i>	<i>0.55</i>
<i>LG13</i>	<i>Santiago Rd Quarry</i>	<i>Qt1 / Santiago</i>	<i>33</i>	<i>lost</i>	<i>--</i>	<i>--</i>	<i>--</i>
<i>LG14</i>	<i>Baker Cyn</i>		<i>25</i>	<i>lost</i>	<i>--</i>	<i>--</i>	<i>--</i>
EG1	22 Freeway Cut	Qal	n.a.	4.2±0.8	n.a.	Holocene	0
EG2	22 Freeway Cut	Qal	n.a.	6.3±1.1	n.a.	Holocene	0

FIGURES

Figure 1 Shaded Digital Elevation Model (DEM) of the southern Los Angeles basin, Orange County, California, and geomorphic indicators of active tectonic deformation. The image was created by tiling together 10 meter USGS DEMs for 1:24,000-scale quadrangles. Key index features referred to in the text, and shown on the image are: CH – Coyote Hills, IR – Irvine Basin, LR – Loma Ridge, NBB – Newport Back Bay (Upper Newport Bay), PH – Puente Hills, PT – Plano Trabuco, SAM – Santa Ana Mountains, SAR – Santa Ana River, SC – Santiago Creek, SJC – San Juan Creek, SJH – San Joaquin Hills. The image reveals many important physiographic indicators of active deformation. For example, the Santa Ana River is forced into a narrow canyon by convergence between the northern Santa Ana Mountains and the eastern Puente Hills (1). The San Joaquin Hills are growing (verging) northward into the Irvine Basin, as shown by the E-W pattern of those streams now entrained in the uplift (2). Sediment from the uplifting Loma Ridge is accumulating against the southern San Joaquin Hills because the SJH uplift has reversed the drainage to the north (3). Santiago Creek and the streams draining the Santa Ana Mountains are trapped between the Santa Ana Mountains and Loma Ridge by the uplift of Loma Ridge, itself being deformed by a series of north-vergent hanging wall faults (4). The Puente Hills are a south verging fold as shown by the linear parallel nature of the southwest flowing stream pattern, a pattern right-laterally offset by the Whittier fault before it can reach the range front (5). The Coyote Hills are deforming sediments deposited in the modern Santa Ana River fan delta by a series of blind thrust ramps (6).

Figure 2 Seismic hazard map of Southern California (SCEC, 1995). Orange County is mostly green, one of the lowest hazard levels in the region.

Figure 3 Photograph of Santa Ana Mountains: Standing east of the Santa Ana Mountains (SAM) and looking westward from Riverside, California, notice SAM dominating left portion of the skyline. The Puente Hills (PH) form the low erosion surface to the right of the Santa Ana River (SAR) water gap.

Figure 4 Tectonic map of northeast part of the southern Los Angeles basin showing the principal faults (red) and geomorphic features. The Elsinore fault is moving the Santa Ana Mountains northward at a rate of 5-6 m/ka. In the northern Santa Ana Mountains, the Elsinore fault bifurcates into the Chino and Whittier faults, with each fault accommodating a portion of the slip. The Chino fault appears to die out to the north. The Whittier fault continues at least 40 km to the northwest where it steps over onto several structures that comprise the Coyote Pass fault and escarpment. Several interpretations exist for the compressional faults (barbed) south of the Puente Hills, but all involve a form of strain partitioning with the Whittier fault. Additional details on these, and other, faults are presented in Table 1 of companion report (Gath et al., 2002). AWF – Alhambra Wash fault, CF – Chino fault, E – Elsinore fault, EMF – El Modena fault, LCF – La Cienega fault, NF – Norwalk fault, PHT – Peralta Hills thrust, S – San Jose fault, WF – Whittier fault. The two primary rivers are also shown: SA – Santa Ana River and SG – San Gabriel River. Modified from Gath (1997).

Figure 5 Location map for samples LG4 and LG5.

Figure 6 Photo of sample location for LG4 and LG5.

Figure 7 Highest (left) and intermediate (right) erosional surfaces in the eastern Puente Hills.

Figure 8 Terrace and Sample Location map in the Santa Ana Canyon. See Figure 12 for more explanation.

Figure 9 Large elevated fill terrace (Terrace 3) in the Santa Ana Canyon (left). Terrace 1 (right) is dominantly conglomeratic, and has a moderately well developed soil profile.

Figure 10 Terrace 2 and Sample Location LG-7 (left) and Terrace 1 (or 2) and Sample Location LG-6 (right).

Figure 11 Terrace 2 surface and Sample Location LG-11. A second sample, LG-10 was contaminated in a lab accident. Sample was obtained from the scarp generated by a road cut slump immediately below the photo.

Figure 12 Terrace 1 (or 2?) and Sample Location LG-8.

Figure 13 Terrace 1 and Sample Location LG-9.

Figure 14 Map of fluvial terraces in Santa Ana Canyon. Five fill terraces and four (three shown) erosional strath surfaces have been recognized and mapped. Preferred ages shown are based on sea level correlation or the soil age estimates of Rockwell and Gath (1988) for the terrace surfaces. Qt3 has been laterally offset by the Whittier fault with no vertical separation of the terrace surface. Four streams that have incised into Qt3 are laterally offset 360-400 meters, indicating a late Quaternary slip rate for the Whittier fault of about 3 mm/yr, conformable with the paleoseismically determined rate (Gath and Rockwell, in prep.; Gath et al 1992;), and yielding good confirmation to the terrace surface age estimate.

Figure 15 – Map of fluvial terraces in Santiago Canyon near Irvine Lake (reservoir).

Figure 16 Terrace Qt2 in Santiago Creek above Irvine Lake, with Santa Ana Mountains in background. Qt2 sample location in gully (LG1, LG2).

Figure 17 Preliminary neotectonic model of the northern Santa Ana Mountains and southern Los Angeles basin, Orange County, California. In this model, partitioned strain off the Newport-Inglewood fault causes uplift of the San Joaquin Hills (SJH). An underlying blind thrust fault (see Shaw and Shearer, 1999) causes uplift of the Puente Hills (PH) and Coyote Hills (CH). The SAM uplift is caused by a partial termination of the Elsinore fault and consumption of slip along a north-vergent blind thrust aligned roughly east-west. The Loma Ridge (LR) uplift is caused by north-vergent strain that is compressing the Tertiary sediments against the uplifting SAM, forming Loma Ridge and deforming Santiago Creek (SC) trapped between them. Arrows indicate direction of motion. Solid red lines are previously mapped strike-slip faults. Dashed red lines are suspected blind thrust faults.

Santiago Creek appears to be displaced by a series of en-echelon faults, indicated by five orange lines.

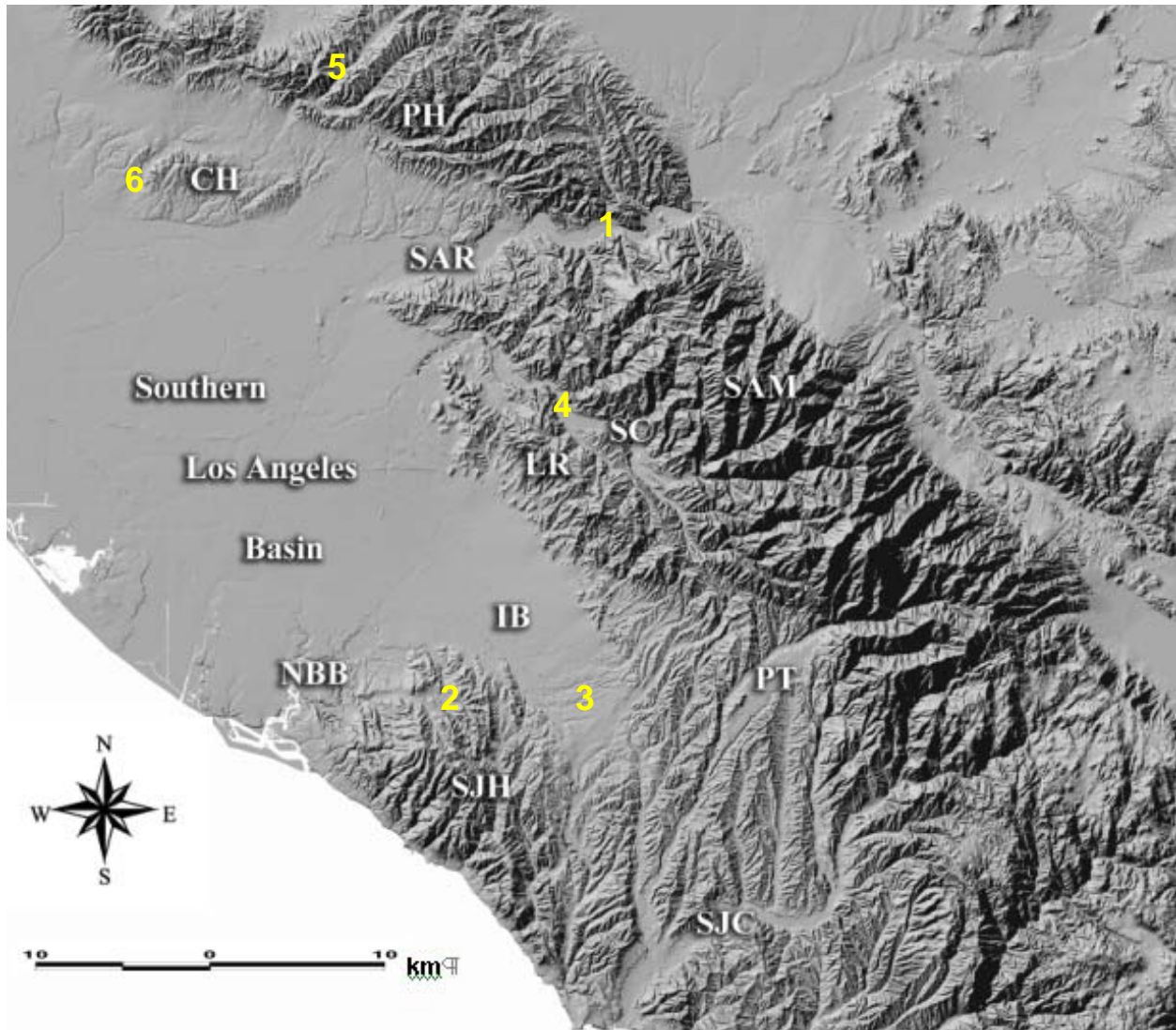


Figure 1: Shaded Digital Elevation Model (DEM) of the southern Los Angeles basin, Orange County, California, and geomorphic indicators of active tectonic deformation. The image was created by tiling together 10 meter USGS DEMs for 1:24,000-scale quadrangles. Key index features referred to in the text, and shown on the image are: CH – Coyote Hills, IR – Irvine Basin, LR – Loma Ridge, NBB – Newport Back Bay (Upper Newport Bay), PH – Puente Hills, PT – Plano Trabuco, SAM – Santa Ana Mountains, SAR – Santa Ana River, SC – Santiago Creek, SJC – San Juan Creek, SJH – San Joaquin Hills. The image reveals many important physiographic indicators of active deformation. For example, the Santa Ana River is forced into a narrow canyon by convergence between the northern Santa Ana Mountains and the eastern Puente Hills (1). The San Joaquin Hills are growing (verging) northward into the Irvine Basin, as shown by the E-W pattern of those streams now entrained in the uplift (2). Sediment from the uplifting Loma Ridge is accumulating against the southern San Joaquin Hills because the SJH uplift has reversed the drainage to the north (3). Santiago Creek and the streams draining the Santa Ana Mountains are trapped between the Santa Ana Mountains and Loma Ridge by the uplift of Loma Ridge, itself being deformed by a series of north-vergent hanging wall faults (4). The Puente Hills are a south verging fold as shown by the linear parallel nature of the southwest flowing stream pattern, a pattern right-laterally offset by the Whittier fault before it can reach the range front (5). The Coyote Hills are deforming sediments deposited in the modern Santa Ana River fan delta by a series of blind thrust ramps (6).

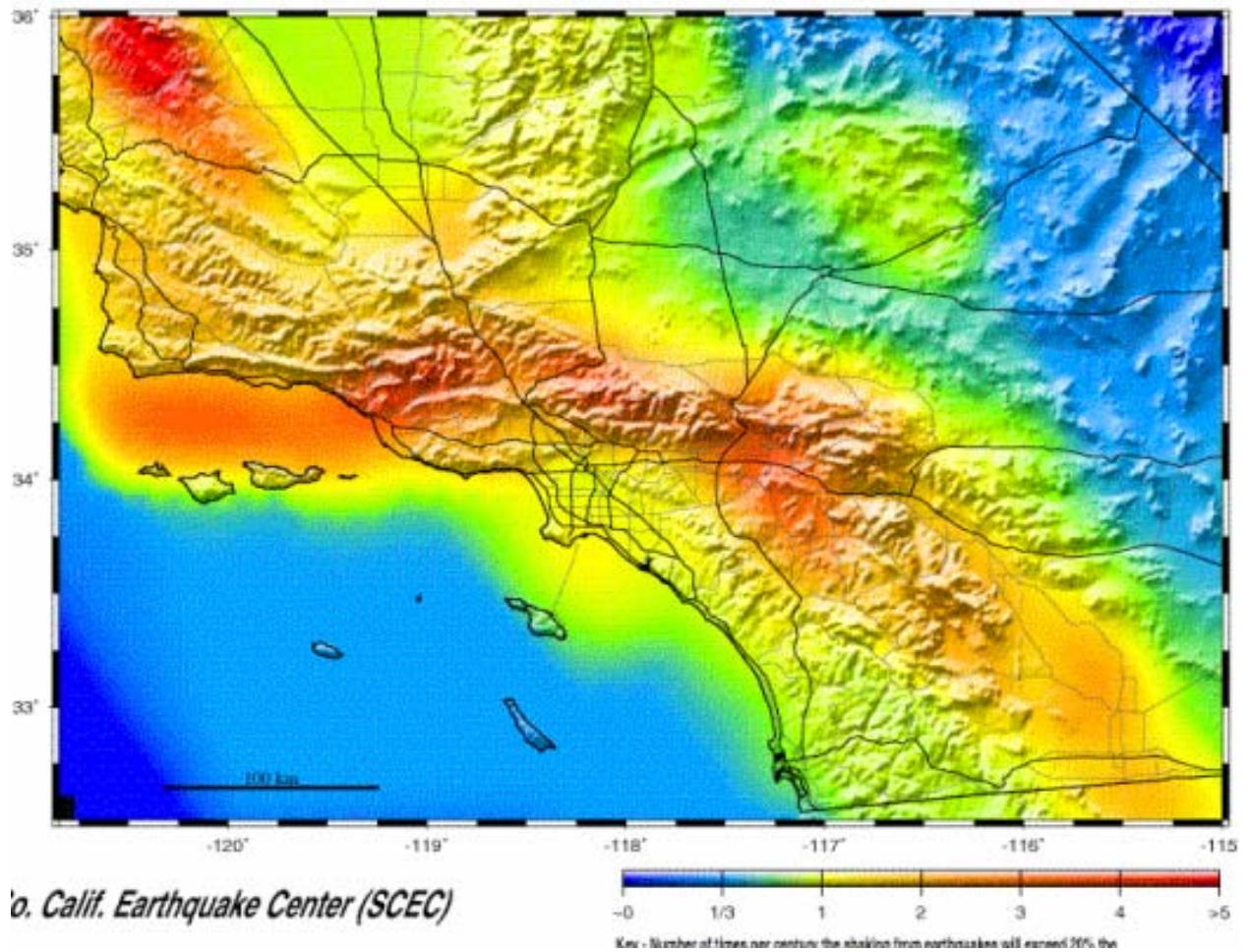


Figure 2: Seismic hazard map of Southern California(SCEC, 1995). Orange County is mostly green, one of the lowest hazard levels in the region.

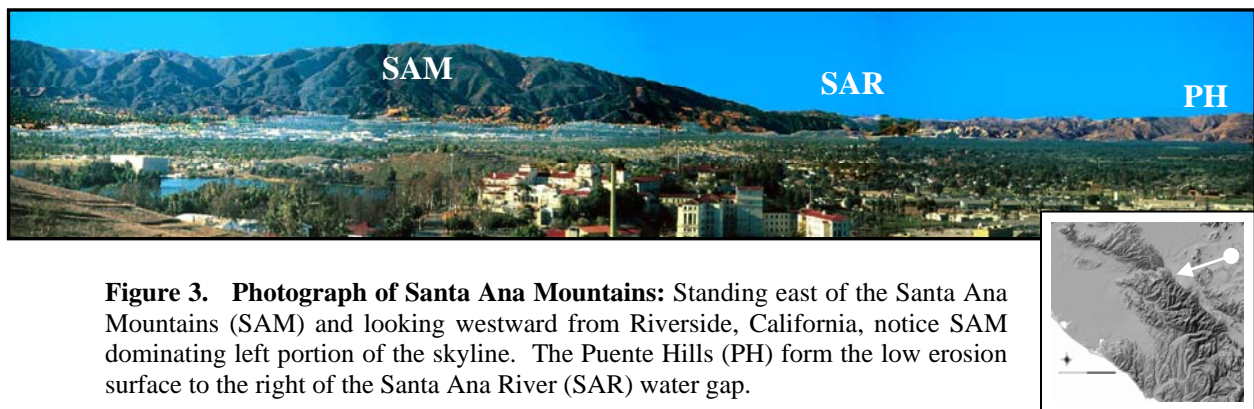




Figure 4: Tectonic map of northeast part of the southern Los Angeles basin showing the principal faults (red) and geomorphic features. The Elsinore fault is moving the Santa Ana Mountains northward at a rate of 5-6 m/ka. In the northern Santa Ana Mountains, the Elsinore fault bifurcates into the Chino and Whittier faults, with each fault accommodating a portion of the slip. The Chino fault appears to die out to the north. The Whittier fault continues at least 40 km to the northwest where it steps over onto several structures that comprise the Coyote Pass fault and escarpment. Several interpretations exist for the compressional faults (barbed) south of the Puente Hills, but all involve a form of strain partitioning with the Whittier fault. Additional details on these, and other, faults are presented in Table 1 of companion report (Gath et al., 2002). AWF – Alhambra Wash fault, CF – Chino fault, E – Elsinore fault, EMF – El Modena fault, LCF – La Cienega fault, NF – Norwalk fault, PHT – Peralta Hills thrust, S – San Jose fault, WF – Whittier fault. The two primary rivers are also shown: SA – Santa Ana River and SG – San Gabriel River. Modified from Gath (1997).



Figure 7: Highest (left) and intermediate (right) erosional surfaces in the eastern Puente Hills.

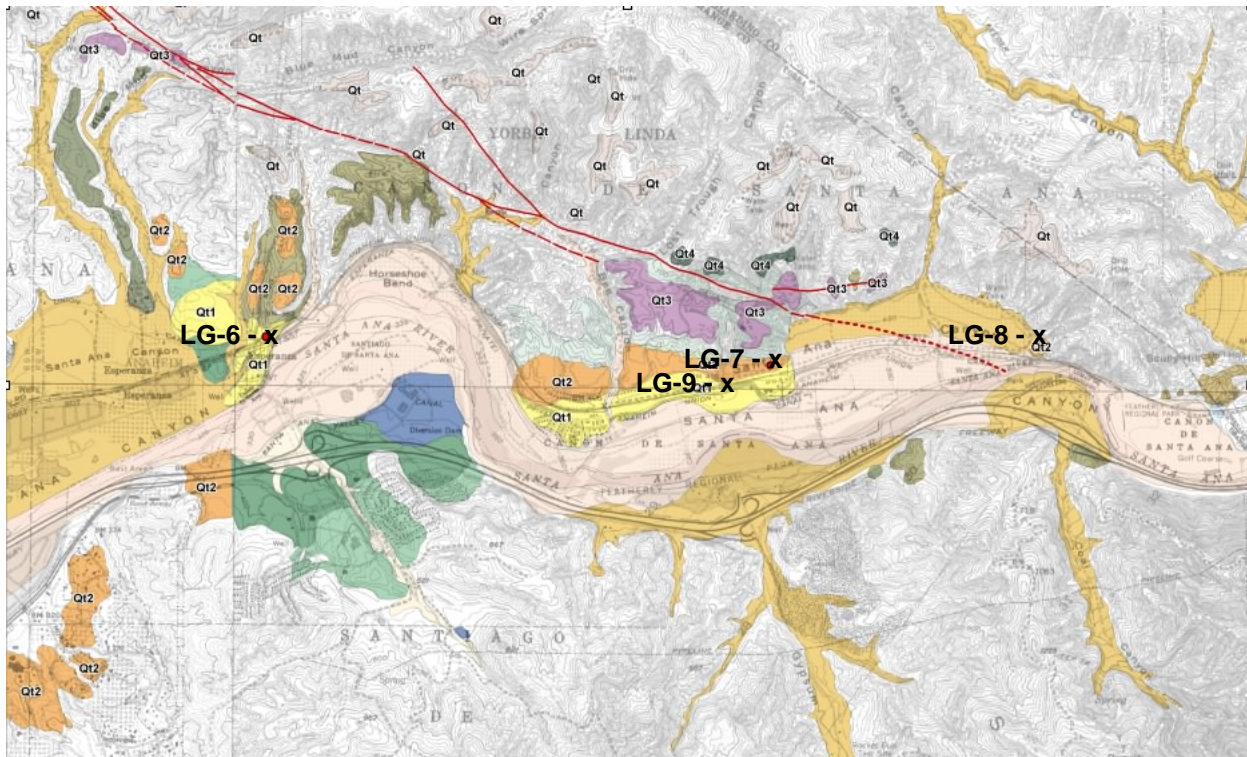


Figure 8: Terrace and Sample Location map in the Santa Ana Canyon. See Figure 14 for more explanation.



Figure 9: Large elevated fill terrace (Terrace 3) in the Santa Ana Canyon (left). Terrace 1 (right) is dominantly conglomeratic, and has a moderately well developed soil profile.



Figure 10: Terrace 2 and Sample Location LG-7 (left) and Terrace 1 (or 2) and Sample Location LG-6 (right).



Figure 11: Terrace 2 surface and Sample Location LG-11. A second sample, LG-10 was contaminated in a lab accident. Sample was obtained from the scarp generated by a road cut slump immediately below the photo.



Figure 12: Terrace 1 (or 2?) and Sample Location LG-8.



Figure 13: Terrace 1 and Sample Location LG-9.

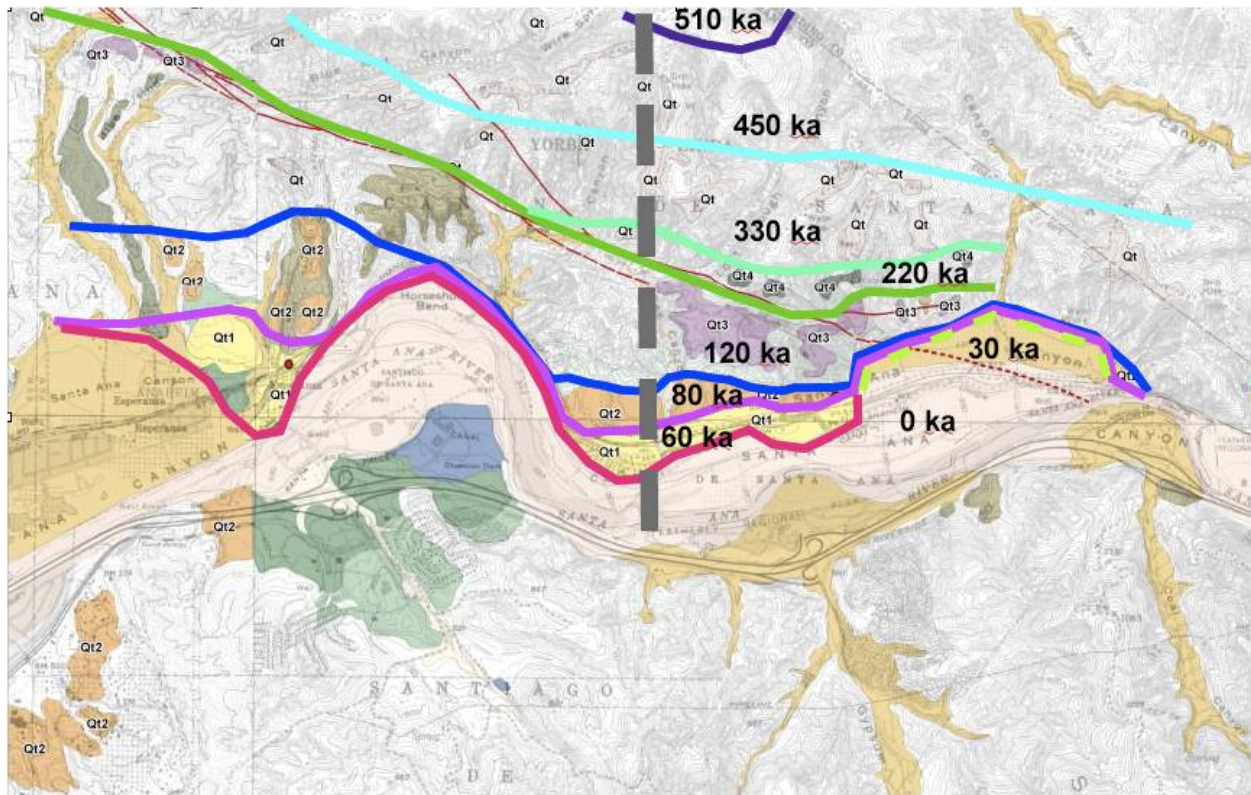


Figure 14 : Map of fluvial terraces in Santa Ana Canyon with preferred ages.

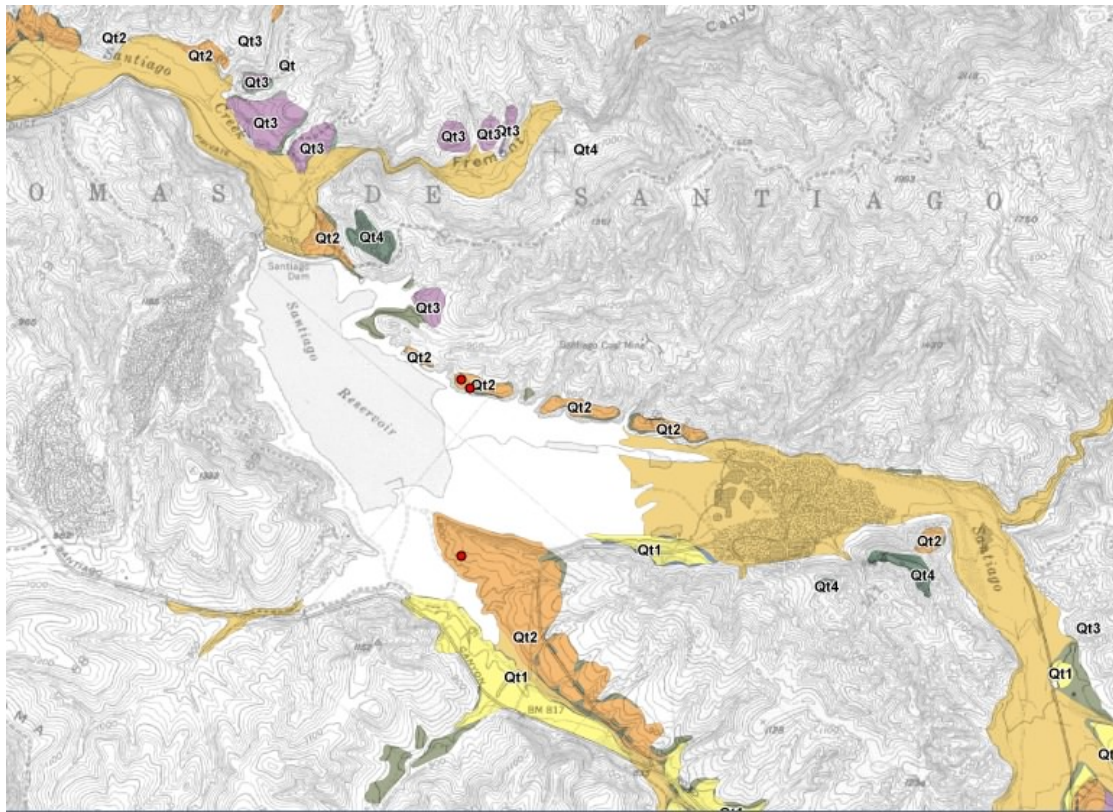


Figure 15 - Map of Santiago Creek terraces at Irvine Lake. OSL sampling locations (LG1, LG2 and LG3) are marked by red dots.

Figure 16 – Terrace Q2 in Santiago Creek above Irvine Lake, with Santa Ana Mountains in background. Samples LG-1 and LG-2 taken from gullies in terrace.



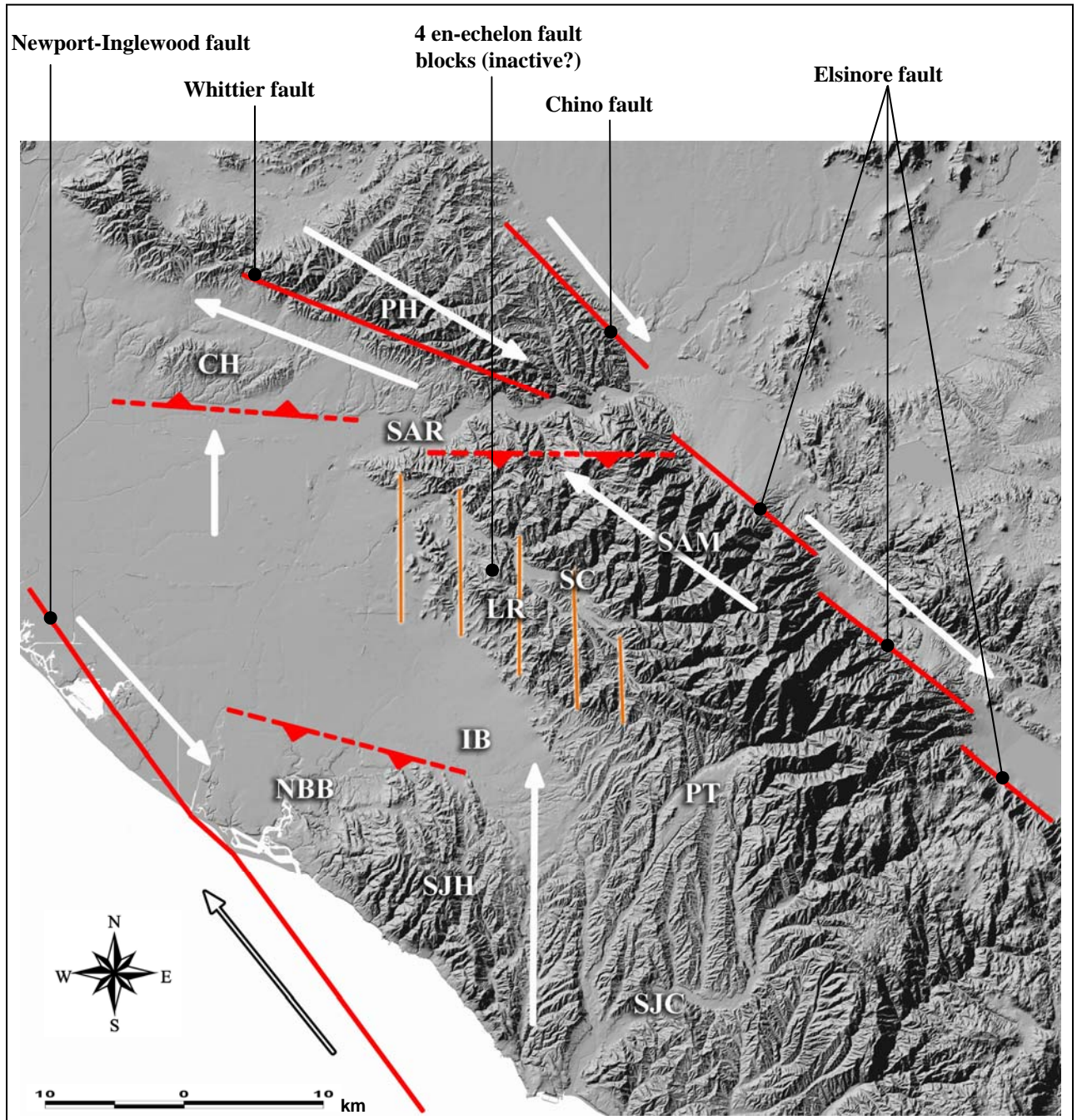


Figure 17